

See discussions, stats, and author profiles for this publication at: <https://www.researchgate.net/publication/231222338>

Turbulence: The Legacy of A.N. Kolmogorov

Book in Astrophysical Letters & Communications · November 1995

DOI: 10.1017/CBO9781139170666

CITATIONS

4,098

READS

5,941

1 author:



Uriel Frisch

Observatoire de la Côte d'Azur

277 PUBLICATIONS 26,663 CITATIONS

[SEE PROFILE](#)

Some of the authors of this publication are also working on these related projects:



Lattice gases [View project](#)



Cauchy-Lagrangian [View project](#)

Frisch #0

LECTURES ON TURBULENCE AND LATTICE GAS HYDRODYNAMICS**Uriel Frisch**

CNRS, Observatoire de Nice
 B.P. 139, 06003 Nice Cedex, France
 e-mail: uriel@froni51.bitnet

*Presented at the Summer School on Turbulence,
 NCAR, Boulder, Colorado, June 1987.*

This set of lectures covers the following topics: fully developed turbulence (#1-2), turbulent transport (#3), large-scale instabilities in flows lacking parity-invariance (#4), lattice gas hydrodynamics (#5-10).

Published in "Lecture Notes on Turbulence"

J.-R. Herring and J. C. McWilliams eds.
 World Scientific 1989

These lectures correspond to
 pp. 219-296.

Frisch #1

CURRENT BELIEFS ABOUT FULLY DEVELOPED TURBULENCE**Part 1**

Lecture 1:

U. Frisch

This and the next lecture are based on material published in French (U. Frisch, Phys. Scr., **9**, 131, 1985) and in English translation (U. Frisch, in "Dynamical systems; a renewal of mechanism", ed. S. Diner, p. 13, World Publish. Co., 1986). To avoid duplication of existing material, the present notes and references remain sketchy. Phenomenological aspects of fully developed turbulence are not covered (see the lectures by H. Tennekes).

Incompressible three dimensional flow is described by the Navier-Stokes (N-S) equations

$$\begin{aligned} \partial_t \mathbf{v} + \mathbf{v} \cdot \nabla \mathbf{v} &= -\nabla p + \nu \nabla^2 \mathbf{v} + \mathbf{f} \\ \nabla \cdot \mathbf{v} &= 0, \end{aligned} \quad (1.1)$$

plus initial and boundary conditions. The Reynolds number, R , is defined as the ratio of the product of the typical length scale, L , times the typical velocity, V , divided by the kinematic viscosity, ν :

$$R = \frac{LV}{\nu}. \quad (1.2)$$

Fully developed turbulence is defined as the behavior obtained in the limit $R \rightarrow \infty$. For example, in astrophysical turbulence a typical value is $R = 10^{12}$. As R tends to infinity the number of effectively excited degrees of freedom in a typical volume scales approximately as $R^{9/4}$.

There are situations, such as statistical mechanics of many interacting particles, where the large numbers of degrees of freedom can be used to greatly simplify the problem. For fully developed turbulence, the hope has been for a long time that a contracted and universal description will be found. By universal one understands a description which is independent of the details of boundary conditions and initial conditions, except for scaling factors.

Nothing of this sort has yet been derived systematically from the N-S equations. There is however experimental evidence for universal laws. For example, the experiment on tidal channel flow with $R = 10^8$ by Grant, Stewart, Moilliet (J. Fluid Mech., **12**, 241, 1962) clearly shows the Kolmogorov -5/3 scaling law for the energy spectrum over three decades (figure 1.1). Experimental data encompassing comparable inertial ranges while taking advantage of modern experimental and data processing techniques have recently been obtained at the Modane wind tunnel by Y. Gagne and E. Hopfinger (Y. Gagne,

Thèse de Doctorat, Institut de Mécanique de Grenoble, 1988). They reveal a power-law somewhat steeper than predicted by the Kolmogorov theory (the exponent is about -1.72).

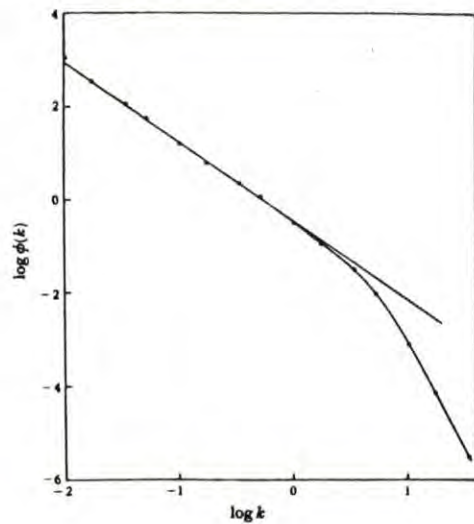


Figure 1.1: A logarithmic plot of one-dimensional energy spectrum. The straight line has a slope of $-5/3$. From Grant, Stewart, and Moilliet (1962).

Understanding universality (or disproving it) without recourse to phenomenology or closure assumptions is a great challenge for the theoreticians. As has been the case in High Energy Physics, the use of the symmetries and conservation laws can shed some light on the issues. This was at the core of Kolmogorov's (C.R. Acad. Sci. USSR, **30**, 301, 1941) derivation of the $-5/3$ law. Much more than dimensional analysis, in the author's view. We shall now present Kolmogorov's argument using such language.

In the absence of forces or boundaries, the N-S equations are invariant under the (non-exhaustive) list of transformations: space and time translations, rotations, planar symmetries, Galilean transformations, and scaling transformations (for $\nu = 0$ or $\nu \rightarrow 0$). The scaling transformations can be parameterized as

$$r \rightarrow \lambda r, \quad v \rightarrow \lambda^h v, \quad t \rightarrow \lambda^{1-h} t, \quad (1.3)$$

where λ is a positive real number, and h is to be determined. The 1941 argument of Kolmogorov (K-41) can be expressed by the following equivalence principle: *In the limit $R \rightarrow \infty$, all invariance properties of the Navier-Stokes equations, possibly broken at large scales by mechanisms generating turbulence, are recovered at small scales in a statistical sense.*

In other words, the flow tries to have maximum symmetry at small scales. The exponent h is determined by the constraint of a constant rate of energy flow from large scales to small scales. Assuming that the flow of energy through a wavenumber k is independent of k , so that it equals the total rate of energy injected at high wavenumbers, fixes h to the value $1/3$. This argument is independent of the details of the energy transfer, whether it is done in small steps or large steps. On dimensional grounds, the energy flux is given by $v v v \nabla$, which behaves like v^3/l . Since this scales as l^{3h-1} and must be independent of l , $h = 1/3$. There is no doubt that the N-S equations admit such scale-invariant solutions, at least formally. It is well known, however, that solutions of nonlinear systems may or may not exhibit the full symmetry of the equations. The symmetry may be *broken* either externally or spontaneously.

An example is given by Burgers equation (Burgers, J.M., *The Nonlinear Diffusion Equation*, Reidel, Boston, 1974)

$$\partial_t u + u \partial_x u = \nu \partial_{xx} u \quad (1.4)$$

which has all the symmetries of the N-S equations, but is integrable. The transformation

$$u = -2\nu \partial_x \log \theta \quad (1.5)$$

changes Burgers equation into the heat equation. As is well known, for $\nu \rightarrow 0$ the solutions of Burgers equation develop shocks which break the scale-invariance. Burgers equation is very useful for "spoiling" the game: most turbulence models which are applied to it do not work! If you have a new idea for fully developed turbulence, try it out on Burgers equation first.

The definition of self-similarity used in the Kolmogorov theory implies that when the flow is viewed with a magnifying glass, placed anywhere, it exhibits always the same structure. This property is not shared by a shock-like solution where all the singularities are concentrated in isolated points. More generally, this definition of self-similarity rules out singularities concentrated on objects which are not space-filling, such as fractals. The latter

are only conditionally self-similar. To take a famous example borrowed from B. Mandelbrot, the fractal nature of the coast of Britain is not revealed if we put a magnifying glass at Canterbury! Kolmogorov's assumed self-similarity has strong implications for moments. For example, the nondimensionalization of the fourth order moment through division by the square of the second order moment should be scale-independent.

Singularities provide one possible mechanism for breaking self-similarity. It is interesting to examine their presence in high Reynolds number flow. An experiment on turbulent flow in a channel exhibits intermittency in the dissipation range (figure 1.2).



Figure 1.2: Signal recorded by an anemometer behind a grid turbulence after high-pass filtering. Data obtained by Y. Gagne (Grenoble).

The turbulent velocity signal was high-pass filtered, with a cutoff frequency in the dissipation range. If the cutoff frequency is too high the signal becomes swamped by the noise. Related intermittent bursts were noticed as early as 1949 by Batchelor and Townsend (Proc. Roy. Soc., A199, 238, 1949). Where does such dissipation range intermittency come from? It has been found that these bursts reflect the fact that the solution has singularities at complex times (Frisch and Morf, Phys. Rev. A23, 2673, 1981). To understand this we make a brief digression into some basic complex analysis.

When solutions of the N-S equation are extended to complex space or time, singularities are unavoidable. An understanding of intermittency can be obtained by examining

the Fourier transform of a function with isolated singularities at complex time-locations $z_j = t_j + i\tau_j$, assumed to be of power-law type:

$$v(z) \sim a_j(z - z_j)^\rho, \quad z \rightarrow z_j, \quad (1.6)$$

where ρ is anything but an integer.

The Fourier transform is given by

$$\hat{v}(w) = \int_R e^{i\omega t} v(t) dt, \quad (1.7)$$

and can be evaluated asymptotically as $\omega \rightarrow \infty$ by Laplace's method (figure 1.3) as

$$\hat{v}(w) \sim \frac{-2 \sin(\pi\rho) \Gamma(\rho + 1)}{\omega^{\rho+1}} e^{-i\pi\rho/2} \sum_j \epsilon_j a_j e^{i\omega z_j}. \quad (1.8)$$

The sum is over singularities with positive imaginary parts. The ϵ_j 's are determination factors.

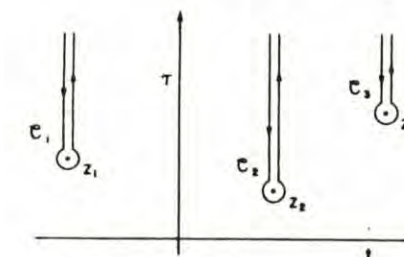


Figure 1.3: Integration contour around singularities in the complex plane. After Frisch and Morf (1981).

The high-pass filtered signal with cutoff $\Omega \rightarrow \infty$ is given by

$$\begin{aligned} v_\Omega(t) &= \frac{1}{2\pi} \int_{|\omega|>\Omega} e^{-i\omega t} \hat{v}(\omega) d\omega \\ &\sim \frac{\Gamma(\rho + 1)}{\Omega^{\rho+1}} \sum_j \epsilon_j a_j e^{-\Omega \tau_j} \operatorname{Re} \left[\frac{\exp(-i\Omega(t - t_j) - i\pi\rho/2)}{t - z_j} \right]. \end{aligned} \quad (1.9)$$

This shows that $v(t)$ has bursts centered at t_j with amplitude proportional to $\exp(-\Omega t_j)$. Since Ω is large, the asymptotic solution picks out singularities closest to the real axis. It turns out that any nonlinear dynamical system generically has singularities in the complex plane. This is not surprising since physical constraints are only strong in the real domain. For example, the energy, as a sum of squares, gives bounded terms on the real axis, but not so in the complex plane where blow-up can occur. Generically, complex singularities translate to bursts. The probe in Gagne's experiment recorded a real signal displaying bursts after high-pass filtering, evidence for singularities in the complex domain.

Nonlinear systems, especially nonintegrable ones, have actually a more complicated singularity structure. Fractal clustering of complex time singularities, rather than isolated singularities (as above) is the rule. Known examples include the Hénon-Heiles system, the time-independent Kuramoto-Sivashinsky equation, and the Arnold-Beltrami-Childress flow. Typically, the solution near a complex singularity is given by an expansion of the form:

$$u \sim (z - z_*)^{-\alpha} F(z - z_*, g_1(z - z_*), g_2(z - z_*), \dots), \quad (1.10)$$

where z_* is the location of the complex time singularity, $F(u, v, w, \dots)$ is an analytic function of its arguments, and the g_i are nonanalytic functions of the form:

$$g_i \sim \begin{cases} (z - z_*)^{\rho_i}, & \rho_i \text{ complex} \\ (z - z_*) \log(z - z_*). \end{cases} \quad (1.11)$$

Complex powers imply that in the neighborhood of a singularity, there are many others; the whole set of singularities generally forms a fractal set.

It is still not known if the singularities of the Navier-Stokes equations do form such a fractal set in the complex domain. Neither is it known if, as $R \rightarrow \infty$, some complex singularities migrate to the real domain. Scaling relations observed in experiments on fully developed turbulence can be interpreted by assuming this to be the case. Let assume that this happens and that the singularities reside on a subset S of \mathbb{R}^3 . S is characterized by its Hausdorff dimension d . The singularities are characterized by a scaling exponent for the velocity:

$$|v(r + l) - v(r)| \sim l^h, \text{ for } r \in S \text{ and } l \rightarrow 0. \quad (1.12)$$

A consequence of this for the structure functions (moments of velocity increments) is:

$$\langle |v(r + l) - v(r)|^p \rangle \sim l^{ph} l^{3-d} \equiv l^{\zeta_p}. \quad (1.13)$$

The l^{ph} comes from the singularity scaling, and the l^{3-d} is the probability that a ball of radius l encounters the set S . In 1941, without using his celebrated self-similarity assumption, Kolmogorov derived directly from the Navier-Stokes equations that the exponent of the third order structure function should be one. Thus $\zeta_3 = 3h + 3 - d = 1$, so that d and h are not independent. If the velocity field is self-similar then $d = 3$, the factor l^{3-d} is unity, and we obtain the standard K-41 result $h = 1/3$.

One way to test this fractal model is to measure the exponents ζ_p and compare with the predicted linear-plus-constant dependence on p . This is difficult because in order to measure high order moments one needs averages over times that grow exponentially with p . In addition, real experiments sample at discrete times, while high order structure functions are dominated by rare, sudden events which may be missed. Figure 1.4 (Anselmet, Gagne, Hopfinger, and Antonia, J. Fluid. Mech., 140, 63, 1984) shows data from several experiments of ζ_p vs. p . It is seen that for low p the data agree with the Kolmogorov scaling, but at high p it may not even be linear.

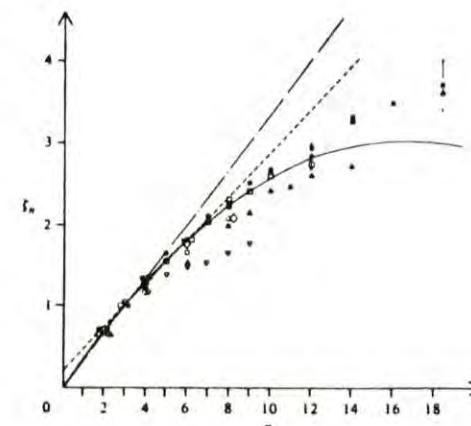


Figure 1.4: Exponent ζ_n of structure function of order n . (n is denoted p in the present text). Figure taken from Anselmet et al.(1984).

The multi-fractal model of Parisi and Frisch (in "Turbulence and predictability in geophysical fluid dynamics and climate dynamics", School Enrico Fermi, Course 88, 1983, p. 84, North Holland, 1985) provides a possible framework for explaining such data. Ex-

ponents falling on a concave curve can be obtained from a set of singularities composed of nested, increasingly singular fractal sets, each with its own dimension and singularity exponent. The evaluation of the structure functions is done as above, but the contributions from the various singular sets must be added with an unknown (and irrelevant) weighting $d\mu(h)$:

$$\langle [v(r+l) - v(r)]^p \rangle \sim \int d\mu(h) l^{ph + 3 - d(h)}. \quad (1.14)$$

As $l \rightarrow 0$ the minimum exponent dominates, resulting in

$$\langle [v(r+l) - v(r)]^p \rangle \sim l^{\zeta_p}, \quad \zeta_p = \min_p(ph + 3 - d(h)). \quad (1.15)$$

Thus, the exponent ζ_p is the Legendre transform of the co-dimension $3 - d(h)$.

Frisch #2

CURRENT BELIEFS ABOUT FULLY DEVELOPED TURBULENCE

Part 2

U. Frisch

Notes by S. Derbyshire and L. M. Polvani

In the previous lecture it was shown that singularities can break the scale-invariance, thereby providing a mechanism for intermittency corrections to the K-41 theory. In 2-D, well known theorems for ideal and viscous fluids rule out the development of real singularities in finite time from a smooth initial field. In 3-D the strongest known mathematical result is that smooth fields remain smooth for at least a short time.

A simple example shows that naive phenomenological arguments can be misleading. Consider the Burgers equation with zero viscosity:

$$\partial_t u + u \partial_x u = 0 \quad (2.1)$$

Under the transformation $w = -\partial_x u$ it may be rewritten in Lagrangian terms:

$$D_t w = w^2, \quad (2.2)$$

to yield:

$$w(t) = \frac{w(0)}{1 - tw(0)}. \quad (2.3)$$

This shows that a singularity will usually develop in finite time. It is tempting to use a similar argument for the 3-D Euler equation in which w is replaced by the vorticity ω . It is a standard result that the vorticity equation can be written in the form:

$$\frac{D\omega}{Dt} = \omega \cdot \nabla u, \quad (2.4)$$

and phenomenologically one *might* estimate the right hand side as the square of the vorticity. With that assumption one obtains:

$$\frac{D\omega}{Dt} \approx \omega^2, \quad (2.5)$$

and therefore

$$\omega(t) \approx \frac{\omega(0)}{1 - t\omega(0)}, \quad (2.6)$$

again leading to a singularity in finite time (at this level of argument the distinction between scalars and vectors is blurred). However evidence is now presented that this need not occur.

The Taylor-Green vortex will provide such an example. The initial velocity distribution is as follows:

$$\begin{aligned} v_1 &= \sin x_1 \cos x_2 \cos x_3 \\ v_2 &= \cos x_1 \sin x_2 \cos x_3 \\ v_3 &= 0. \end{aligned} \quad (2.7)$$

It consists of layers of circular eddies, with those at $x_3 = \pi$ counter-rotating relative to the ones at $x_3 = 0$. For $t > 0$ the flow develops a non-vanishing v_3 component. The evolution of this field under the Euler equations ($\nu = 0$) was solved numerically by Brachet, Meiron, Orszag, Nickel, Morf, and Frisch (J. Fluid Mech., 130, 411, 1983) using a pseudo-spectral method with a resolution of 256^3 grid points.

By arguments similar to the ones presented in the previous lecture, it can be shown that in the presence of singularities in the complex space \mathbf{C}^3 , the energy spectrum defined as:

$$E(t, K) = \sum_{K-1 \leq |\mathbf{k}| < K} |\hat{\mathbf{v}}(t, \mathbf{k})|^2 \quad (2.8)$$

has the asymptotic behaviour:

$$E(t, K) \propto e^{-2\delta(t)K}, \quad K \rightarrow \infty, \quad (2.9)$$

to within an algebraic prefactor, determined by the nature of the singularities closest to the real domain \mathbf{R}^3 . $\delta(t)$ is called the width of the analyticity band. Such exponential behaviour is indeed seen in the data of Brachet et al. (figure 2.1).

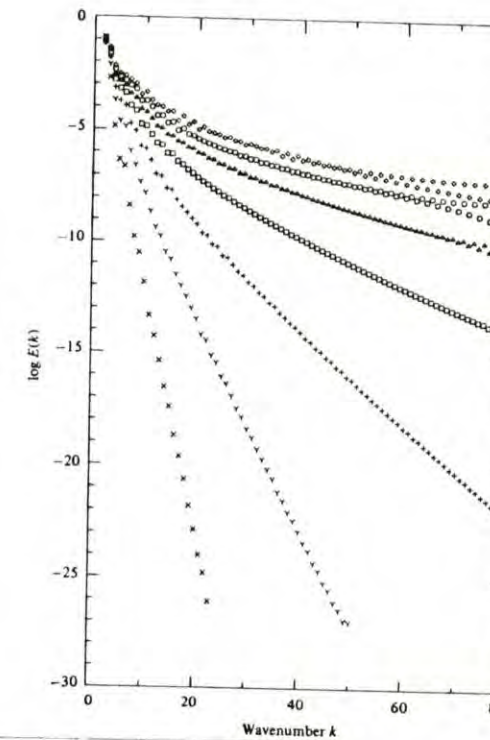


Figure 2.1: The inviscid spectrum $E(k, t)$ for the Taylor-Green vortex. Lin-log scales make exponentials appear as straight lines. The different symbols distinguish the spectra at equally spaced times from crosses at $t = 0.5$ to diamonds at $t = 3.5$ in steps of 0.5. From Brachet et al. (1983).

At each time the value of δ can be estimated from the slopes in figure 2.1, using the asymptotic form given in eq. (2.9). The results are plotted in figure 2.2.

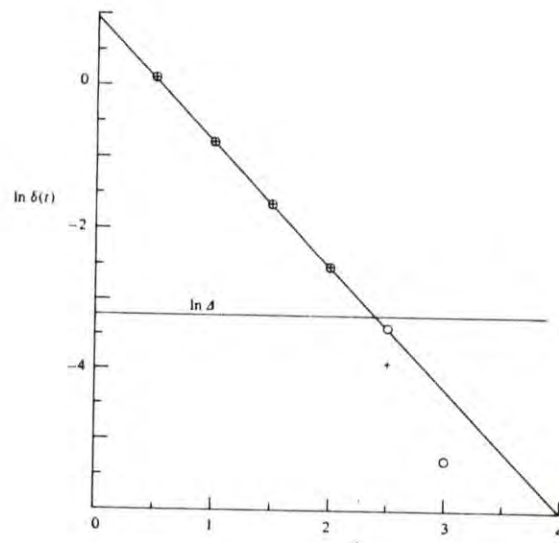


Figure 2.2: The time dependence of the width of the analyticity strip δ for the inviscid Taylor-Green vortex. From Brachet et al. (1983).

By extrapolation the graph suggests that the singularity will take an infinitely long time to reach the real axis. This shows that the analogy with Burgers equation fails in this case. In practice the truncation errors invalidate the solution when $\delta \leq 2\pi/K_{max}$, where K_{max} is the maximum wave-number, but there are sufficient “good” points to make credible decreasing exponential behaviour in $\delta(t)$. The simulation of Brachet et al. suggests a physical reason for the failure of the analogy, namely the formation of pancakes with strongly reduced nonlinearities; this may be a generic property of 3-D flows. Figure 2.3 illustrates this by showing successive stages of the evolution of the inviscid Taylor-Green vortex, at $t = 0$ and $t = 2$.

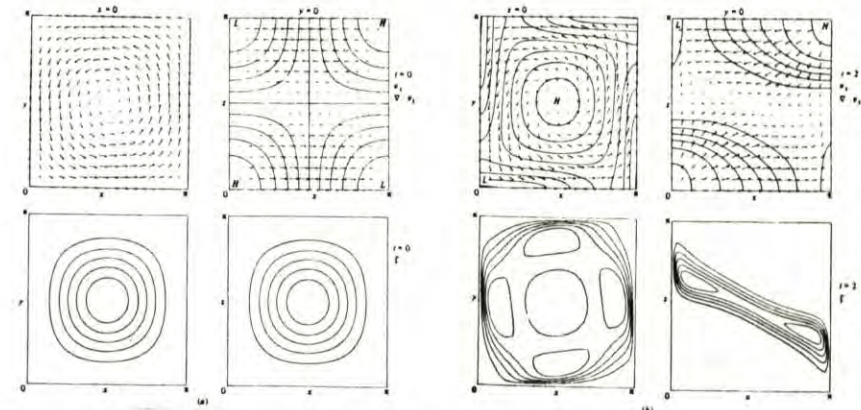


Figure 2.3: Various features for the inviscid Taylor-Green flow, at $t = 0$, (a); and $t = 2.0$, (b). For details, see Brachet et al. (1983).

Another example is provided by the 2-D MHD problem studied by Frisch, Pouquet, Sulem, and Meneguzzi (J. Méc. Théor. Appliqu., special issue on “Two-dimensional turbulence”, p. 191, 1983). The equations are (ω and j are the curl of v and b , respectively):

$$\begin{aligned} \partial_t \omega + \mathbf{v} \cdot \nabla \omega &= \mathbf{b} \cdot \nabla j \\ \partial_t \mathbf{b} + \mathbf{v} \cdot \nabla \mathbf{b} &= \mathbf{b} \cdot \nabla \mathbf{v} \\ \nabla \cdot \mathbf{v} &= 0, \quad \nabla \cdot \mathbf{b} = 0. \end{aligned} \tag{2.10}$$

Note that despite the two-dimensionality, vorticity is not conserved, since it can be generated by the Lorentz force. Phenomenological arguments and even quite sophisticated closures predict finite-time singularities (from smooth initial conditions). However, there is numerical evidence for the formation of quasi-one-dimensional sheets (figure 2.4).

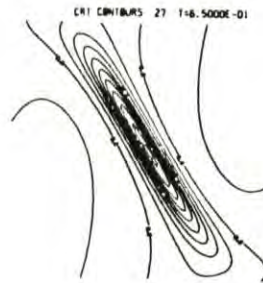


Figure 2.4: Current contours for two-dimensional ideal MHD flow. See Frisch et al. (1983) for details.

To summarize: there is overwhelming evidence for complex singularities, coming arbitrarily close to the real axis in the inviscid (Euler) case. It is widely believed that viscosity prevents any real singularity developing in the Navier-Stokes equations in finite time, but it is not known in general whether finite-time real singularities develop in inviscid flow. However, in the Taylor-Green problem, straightforward extrapolation suggests that such singularities may be absent.

The presence of singularities close to the real axis would raise questions about the validity of hydrodynamics, i.e., the continuum approximation. Leray (Acta Math. **63**, 193, 1934) suggested this as a source of randomness in turbulence. To derive hydrodynamics, one assumes the molecular mean free path λ to be much smaller than the smallest macroscopic-flow scale δ . Physically, following the ideas of K-41, we identify δ with the dissipation scale, and write

$$L_0/\delta \sim R^{3/4} \quad (2.11)$$

where L_0 is the integral ('large') scale for the turbulence. We evaluate the ratio λ/δ as follows:

$$\frac{\lambda}{\delta} = \frac{\lambda}{L_0} \frac{L_0}{\delta} \sim \frac{\lambda}{L_0} R^{3/4} \sim \frac{\lambda}{L_0} \left(\frac{L_0}{\lambda} \frac{V_0}{V_{th}} \right)^{3/4} \sim \left(\frac{\lambda}{L_0} \right)^{1/4} \left(\frac{V_0}{V_{th}} \right)^{3/4}. \quad (2.12)$$

It is here assumed that the kinematic viscosity ν can be estimated as $\nu \sim V_{th} \cdot \lambda$, where V_{th} is the thermal velocity of molecules. Note that V_0/V_{th} is approximately the Mach

number, which must be small for incompressibility to hold, and therefore, unless K-41 is very strongly violated, the hydrodynamic approximation appears valid even in the limit of high Reynolds number.

It is now commonly believed, following the work of Lorenz and others, that the source of randomness in turbulence is the intrinsic stochasticity of the Navier-Stokes equations in certain regimes, i.e., 'deterministic chaos'. The flow-field is thought to evolve towards some attractor, with sensitive dependence on initial conditions. Large-time behaviour would then appear random. One might hope that statistical properties of the system would still be predictable. However, usually in such dynamical systems there exists *more than one attractor*, and the geometry of the basins of attraction may be so complicated as to make even the statistical properties sensitively dependent on initial conditions. The problem of determining the ultimate attractor for each initial point, say, with rational coordinates, may not even be amenable to any finite algorithm.

We cannot rule out, indeed, that some of the central questions of turbulence (as they used to be formulated) are undecidable, in the sense of Gödel and Turing. If this is true, it just indicates that we are on the wrong path by insisting on a purely deterministic description of turbulence. Random perturbations, from external action or from thermal fluctuations, are not only hard to avoid in real flow, they may be essential to avoid the pitfall of "byzantine complexity" (undecidability).

Frisch #3

TURBULENT TRANSPORT OF SCALARS AND MAGNETIC FIELDS

Lecture 3:

U. Frisch

Notes by M. Montgomery, G. Coleman

The purpose of this lecture is to demonstrate the technique of multiple scale analysis as applied to advection of passive scalars (e.g. temperature fields) and vectors (e.g. magnetic fields). Both in turn demonstrate the effect of eddy features on the large scale flow. These techniques are useful for deriving eddy diffusivities and other transport coefficients related to more exotic effects, such as the α -effect in MHD and the AKA (anisotropic kinetic alpha) effect to be discussed in the next lecture. The exposition for the scalar field follows closely a paper by Papanicolaou and Pironneau [1]. The material on the transport of magnetic fields and the α -effect does not incorporate any background material or references. Such material may be found in the monographs by Moffatt [2] and by Zeldovich et al. [3].

1. TRANSPORT OF SCALAR FIELDS

We begin this study of "macrodynamics," the dynamics of large scales, by considering the diffusion of a scalar in an incompressible 2-D or 3-D flow. The flow domain consists of a space-time periodic array of cells whose periodicity equals ℓ in both x_1 , x_2 , and x_3 . The (prescribed) flow velocity within the cells is denoted by \mathbf{u} and satisfies the incompressibility condition $\nabla \cdot \mathbf{u} = 0$. Furthermore, the spatial-temporal average of the flow over a cell, $\langle \mathbf{u} \rangle$, is assumed to vanish and the characteristic value of \mathbf{u} is denoted V .

Observing the domain at macroscopic scales, we address the question of whether or not a superimposed passively advected scalar contaminant of scale size $L \gg \ell$ will undergo diffusion. This situation is analogous to the *turbulent* transport of a passive scalar, except that a space-time periodicity, rather than random homogeneity and stationarity, have been assumed for simplicity. In the latter random case the formalism is essentially unchanged, but there are some mathematical fine points [1]. We note that when the eddy field \mathbf{u} is time-independent and the molecular diffusivity vanishes, the scalar may not diffuse but simply "swirl around" with the flow within each periodic cell. This pathology disappears as soon as a finite molecular diffusivity is introduced.

The governing equation for the concentration Θ of the advected scalar is

$$\partial_t \Theta + \mathbf{u} \cdot \nabla_x \Theta = \kappa \nabla_x^2 \Theta. \quad (3.1)$$

We are interested in the behavior on scales L such that $\frac{\ell}{L} = \epsilon \ll 1$. Simple physical reasoning suggests that there may be an eddy-diffusivity (isotropic or anisotropic) of order

ℓV which is independent of ϵ . Then, the characteristic time scale associated with the large scale should be of order $\frac{\ell^2}{\ell V} = (\frac{\ell}{L})^2 (\frac{\ell}{V}) = \epsilon^{-2} t_{\text{eddy}}$. The simplest way to deal with this situation is to use a multiscale expansion in which we keep both "slow" and "fast" variables. The fast variables are x and t while the slow variables are $X = \epsilon x$ and $T = \epsilon^2 t$. By its definition, the velocity \mathbf{u} depends only on the fast variables and Θ depends on both fast and slow variables. Accordingly, Θ is expanded in powers of ϵ :

$$\Theta(x, X, t, T) = \Theta^{(0)} + \epsilon \Theta^{(1)} + \epsilon^2 \Theta^{(2)} + \dots, \quad (3.2)$$

where all the $\Theta^{(n)}$ depend on x , X , t , and T . It is convenient to decompose $\Theta^{(0)}$ as $\Theta^{(0)} = \langle \Theta^{(0)} \rangle + \tilde{\Theta}^{(0)}$, where $\langle \Theta^{(0)} \rangle$ is the space-time average over the cell, depending only on X and T and $\tilde{\Theta}^{(0)}$ are the fluctuations. The standard multiscale technique pretends that x , X , t , and T are each independent variables to accommodate the substitution of $\Theta(x, X, t, T)$ for $\Theta(x, t)$. So, we employ the chain rule to obtain:

$$\nabla_x \leftarrow \nabla_x + \epsilon \nabla_X \quad (3.3a)$$

$$\partial_t \leftarrow \partial_t + \epsilon^2 \partial_T. \quad (3.3b)$$

Using (3.3) and substituting into (3.1) yields

$$(\partial_t + \epsilon^2 \partial_T) \Theta + \mathbf{u} \cdot (\nabla_x + \epsilon \nabla_X) \Theta = \kappa (\nabla_x + \epsilon \nabla_X)^2 \Theta. \quad (3.4)$$

Inserting the expansion (3.2) into the PDE (3.4) and identifying the powers of ϵ gives a hierarchy of equations, the first of which is:

$$O(\epsilon^0): \quad \partial_t \tilde{\Theta}^{(0)} + \mathbf{u} \cdot \nabla_x \tilde{\Theta}^{(0)} = \kappa \nabla_x^2 \tilde{\Theta}^{(0)}. \quad (3.5a)$$

The solution $\tilde{\Theta}^{(0)}$ is easily shown to go to zero on a fast time scale (see Appendix). Therefore we lose no generality by equating it to zero. The next two equations in the hierarchy are:

$$O(\epsilon): \quad \partial_t \Theta^{(1)} + \mathbf{u} \cdot \nabla_x \Theta^{(1)} = -\mathbf{u}(x, t) \cdot \nabla_X \langle \Theta^{(0)} \rangle + \kappa \nabla_x^2 \Theta^{(1)} \quad (3.5b)$$

$$O(\epsilon^2): \quad \partial_t \Theta^{(2)} + \mathbf{u} \cdot \nabla_x \Theta^{(2)} = -\partial_T \langle \Theta^{(0)} \rangle - \mathbf{u}(x, t) \cdot \nabla_X \Theta^{(1)} + \kappa \nabla_x^2 \Theta^{(2)} + \kappa \nabla_x^2 \langle \Theta^{(0)} \rangle + 2\kappa \nabla_X \cdot \nabla_x \Theta^{(1)}. \quad (3.5c)$$

At first sight this hierarchy seems to imply a closure problem since in the above two equations we have three unknowns. Actually, equations (3.5b,c) will yield a closed

equation for $\langle \Theta^{(0)} \rangle$ via a solvability condition. In many perturbation expansions one encounters Fredholm alternatives, that is equations of the form $Af = g$ where the linear operator A is non-invertible, so that g has to be orthogonal to the null-space of the adjoint of A . Here, in spite of having partial differential operators, the structure is quite straightforward: we notice that all the underlined terms in equations (3.5b,c) have vanishing space-time averages since they are, or might be put in the form of, exact derivatives with respect to one of the fast variables. Thus the sum of all underlined terms must vanish. This plays the role of the usual solvability condition. All the terms of equation (3.5b) have vanishing average and therefore do not provide a solvability condition. The solvability condition is furnished by (3.5c) and reads (summation of repeated indices henceforth understood)

$$\partial_T \langle \Theta^{(0)} \rangle + \frac{\partial}{\partial X_i} \langle u_i \Theta^{(1)} \rangle = \kappa \nabla_X^2 \langle \Theta^{(0)} \rangle. \quad (3.6)$$

The equation for the mean field is closed once $\Theta^{(1)}$ is determined from equation (3.5b). The solution to equation (3.5b) is obtained by noting that it is a PDE in fast variables x and t and that the quantity $\mathbf{G} = \nabla_X \Theta^{(0)}$ is independent of x and t , and thus is a constant as far as integration of the equation is concerned. Furthermore, since equation (3.5b) is linear in $\Theta^{(1)}$, the solution for $\Theta^{(1)}$ can be expressed as

$$\Theta^{(1)} = \chi(\mathbf{x}, t) \cdot \mathbf{G}, \quad (3.7a)$$

where the vector χ satisfies the auxilliary equation:

$$\partial_t \chi + \mathbf{u} \cdot \nabla_x \chi = -\mathbf{u} + \kappa \nabla_x^2 \chi. \quad (3.7b)$$

Substituting (3.7a) into the evolution equation for the mean field renders it closed. The result is

$$\partial_T \langle \Theta^{(0)} \rangle = \left(\kappa \nabla_X^2 + D_{ij} \frac{\partial^2}{\partial X_i \partial X_j} \right) \langle \Theta^{(0)} \rangle, \quad (3.8a)$$

with an eddy diffusivity tensor

$$D_{ij} = -\frac{1}{2} [\langle u_i \chi_j \rangle + \langle u_j \chi_i \rangle]. \quad (3.8b)$$

We note that equation (3.8) represents a diffusion equation for the mean field $\langle \Theta^{(0)} \rangle$ whose diffusivity tensor may be anisotropic. This of course reflects the trivial fact that the flow is usually not invariant under arbitrary rotations. It is enough for the cellular flow

above to be invariant under permutations of the coordinates to insure isotropy of second order tensors and thereby the isotropy of the eddy diffusivity.

The diffusivity tensor is shown to be positive definite by multiplying each component i of equation (3.7b) by χ_j , averaging over a cell, adding the expression obtained by interchanging i and j , and integrating by parts. Thus, $D_{ij} = \kappa \langle \partial_i \chi_i \partial_j \chi_j \rangle$, an obviously positive definite expression. This implies that the passive scalar cannot undergo amplification (which would also violate the maximum principle).

In the special case when the molecular diffusivity κ vanishes, equation (3.7b) may be integrated in "Lagrangian coordinates" to yield (a denotes the starting point and the superscript L refers to Lagrangian coordinates)

$$\chi^L(a, t) = - \int_0^t \mathbf{u}^L(a, t') dt' + \text{const}, \quad (3.9)$$

so that D_{ij} becomes

$$D_{ij} = \frac{1}{2} \int_0^t [\langle u_i^L(a, t) u_j^L(a, t') \rangle + i \leftrightarrow j] dt'. \quad (3.10)$$

For large times and when the integral converges, this is just G.I. Taylor's expression for the eddy-diffusivity as the time-integral of the Lagrangian velocity autocorrelation function.

Here a word of caution is required. In the absence of molecular diffusivity the large-scale dynamics need not be diffusive. Indeed, the study of the nondiffusive advection of a passive scalar is just equivalent to the study of the ODE for the Lagrangian trajectories of fluid particles:

$$\frac{d\mathbf{x}}{dt} = \mathbf{u}(\mathbf{x}, t). \quad (3.11)$$

Since we assume $\nabla \cdot \mathbf{u} = 0$, (3.11) constitutes a *conservative dynamical system* (volume preserving). Such systems have been extensively studied and are known to often develop structures called Kolmogorov Arnold Moser (KAM) surfaces which prevent diffusion! We shall not dwell on such frontier questions [4-5]. With nonvanishing molecular diffusivity the problem seems to dissolve. However, it will reappear if we ask about the behavior of the eddy diffusivity as $\kappa \rightarrow 0$.

The case of finite molecular diffusivity does not lead to such mathematical fine points: the existence of a finite eddy diffusivity is generally guaranteed, but its value cannot be found without solving the auxilliary equation (3.7b). This can be done numerically; since there is no ϵ left in the equation, there is a single time scale, so that the problem is

not “stiff”. Alternatively, the equation can be solved in a low Peclet number (large κ) expansion or in a short correlation-time expansion when the field \mathbf{u} is random. We shall not carry out such expansions here and just mention that, to leading order, the expression for the eddy diffusivity does not involve the *helicity* of the flow, but higher order corrections do.

2. TRANSPORT OF A MAGNETIC FIELD

We shall now demonstrate how the above method must be modified to study the evolution of a magnetic field embedded in the 3-D periodic array described in section 1. The governing equations describing the evolution of a magnetic field in the MHD magnetic regime are (see D. Montgomery’s lectures for explanation of the magnetic regime):

$$\partial_t \mathbf{b} + \mathbf{u} \cdot \nabla_{\mathbf{z}} \mathbf{b} - \mathbf{b} \cdot \nabla_{\mathbf{z}} \mathbf{u} = \lambda \nabla_{\mathbf{z}}^2 \mathbf{b} \quad (3.12a)$$

$$\nabla_{\mathbf{z}} \cdot \mathbf{u} = 0, \quad \nabla_{\mathbf{z}} \cdot \mathbf{b} = 0. \quad (3.12b)$$

We note that the term $\mathbf{b} \cdot \nabla \mathbf{u}$ has no analogue in the scalar advection equation. It turns out that this new term can induce instabilities by stretching the magnetic field. If this happens, we say that we have a “dynamo.”

If we anticipate an “eddy diffusivity” of order one, then the same steps presented in section 1 can be applied to (3.12a) to produce:

$$(\partial_t + \epsilon^2 \partial_T) \mathbf{b} + \mathbf{u} \cdot (\nabla_{\mathbf{z}} + \epsilon \nabla_X) \mathbf{b} - \mathbf{b} \cdot (\nabla_{\mathbf{z}} + \epsilon \nabla_X) \mathbf{u} = \lambda (\nabla_{\mathbf{z}} + \epsilon \nabla_X)^2 \mathbf{b} \quad (3.13a)$$

As before, we expand the magnetic field

$$\mathbf{b}(\mathbf{z}, X, t, T) = \langle \mathbf{b}^{(0)} \rangle + \tilde{\mathbf{b}}^{(0)} + \epsilon \mathbf{b}^{(1)} + \epsilon^2 \mathbf{b}^{(2)} \dots \quad (3.13b)$$

where $\langle \mathbf{b}^{(0)} \rangle$ depends only on the slow variables and all the other $\mathbf{b}^{(n)}$ ’s depend on both fast and slow variables. Expanding, we obtain the following hierarchy:

$$O(\epsilon^0): \quad \underline{\partial_t \tilde{\mathbf{b}}^{(0)}} + \underline{\mathbf{u} \cdot \nabla_{\mathbf{z}} \tilde{\mathbf{b}}^{(0)}} = \tilde{\mathbf{b}}^{(0)} \cdot \nabla_{\mathbf{z}} \mathbf{u} + \langle \mathbf{b}^{(0)} \rangle \cdot \nabla_{\mathbf{z}} \mathbf{u} + \lambda \nabla_{\mathbf{z}}^2 \tilde{\mathbf{b}}^{(0)}, \quad (3.14a)$$

$$\begin{aligned} O(\epsilon): \quad & \underline{\partial_t \mathbf{b}^{(1)}} + \underline{\mathbf{u} \cdot \nabla_{\mathbf{z}} \mathbf{b}^{(1)}} + \underline{\mathbf{u} \cdot \nabla_X \langle \mathbf{b}^{(0)} \rangle} + \underline{\mathbf{u} \cdot \nabla_X \tilde{\mathbf{b}}^{(0)}} \\ & = \mathbf{b}^{(1)} \cdot \nabla_{\mathbf{z}} \mathbf{u} + \lambda \nabla_{\mathbf{z}}^2 \mathbf{b}^{(1)} + 2 \lambda \nabla_{\mathbf{z}}^2 \tilde{\mathbf{b}}^{(0)} \end{aligned} \quad (3.14b)$$

$$O(\epsilon^2): \quad \underline{\partial_t \mathbf{b}^{(2)}} + \underline{\partial_T \tilde{\mathbf{b}}^{(0)}} + \underline{\mathbf{u} \cdot \nabla_{\mathbf{z}} \mathbf{b}^{(2)}} + \underline{\mathbf{u} \cdot \nabla_X \mathbf{b}^{(1)}} \quad (3.14c)$$

$$= -\partial_T \langle \mathbf{b}^{(0)} \rangle + \mathbf{b}^{(2)} \cdot \nabla_{\mathbf{z}} \mathbf{u} + \lambda \nabla_X^2 \langle \mathbf{b}^{(0)} \rangle + 2 \lambda \nabla_{\mathbf{z}}^2 \mathbf{b}^{(1)} + \lambda \nabla_{\mathbf{z}}^2 \mathbf{b}^{(2)}. \quad (3.14c)$$

In addition, we have the expanded forms of the solenoidality condition:

$$\nabla_{\mathbf{z}} \cdot \tilde{\mathbf{b}}^{(0)} = 0, \quad (3.14a')$$

$$\nabla_{\mathbf{z}} \cdot \mathbf{b}^{(1)} + \nabla_X \cdot \tilde{\mathbf{b}}^{(0)} = 0, \quad \nabla_{\mathbf{z}} \cdot \langle \mathbf{b}^{(0)} \rangle = 0, \quad (3.14b')$$

$$\nabla_{\mathbf{z}} \cdot \mathbf{b}^{(2)} + \nabla_X \cdot \mathbf{b}^{(1)} = 0. \quad (3.14c')$$

The underlined terms in (3.14) have zero fast variable average. In order for the system (3.14) to be consistent, two solvability conditions must be satisfied:

$$\langle \mathbf{u} \cdot \nabla_X \tilde{\mathbf{b}}^{(0)} \rangle = 0 \quad (3.15a)$$

$$\partial_T \langle \mathbf{b}^{(0)} \rangle + \langle \mathbf{u} \cdot \nabla_{\mathbf{z}} \mathbf{b}^{(1)} \rangle - \langle \mathbf{u} \nabla_{\mathbf{z}} \cdot \mathbf{b}^{(1)} \rangle = \lambda \nabla_X^2 \langle \mathbf{b}^{(0)} \rangle. \quad (3.15b)$$

(3.15a, b) are obtained by averaging equations (3.14b, c) respectively. The $-\langle \mathbf{u} \nabla_{\mathbf{z}} \cdot \mathbf{b}^{(1)} \rangle$ term in (3.15b) comes from manipulating the $\mathbf{b}^{(2)} \cdot \nabla_{\mathbf{z}} \mathbf{u}$ term in (3.15c) through the solenoidality condition (3.14c’).

Substituting $\mathbf{a} = \mathbf{u}$ and $\mathbf{b} = \tilde{\mathbf{b}}^{(0)}$ into the vector identity

$$\nabla \times (\mathbf{a} \times \mathbf{b}) = (\mathbf{b} \cdot \nabla) \mathbf{a} - (\mathbf{a} \cdot \nabla) \mathbf{b} - (\nabla \cdot \mathbf{a}) \mathbf{b} + (\nabla \cdot \mathbf{b}) \mathbf{a}$$

gives

$$\nabla_X \times (\mathbf{u} \times \tilde{\mathbf{b}}^{(0)}) = -(\mathbf{u} \cdot \nabla_X) \tilde{\mathbf{b}}^{(0)}$$

since \mathbf{u} is independent of X . The solvability conditions can thus be recast as

$$\nabla_X \times \langle \mathbf{u} \times \tilde{\mathbf{b}}^{(0)} \rangle = 0 \quad (3.16a)$$

$$\partial_T \langle \mathbf{b}^{(0)} \rangle = \nabla_X \times \langle \mathbf{u} \times \mathbf{b}^{(1)} \rangle + \lambda \nabla_X^2 \langle \mathbf{b}^{(0)} \rangle \quad (3.16b)$$

A physical interpretation for (3.16) can be obtained by rewriting (3.12) in the form:

$$\partial_t \mathbf{b} = \nabla_{\mathbf{z}} \times (\mathbf{u} \times \mathbf{b}) + \lambda \nabla_{\mathbf{z}}^2 \mathbf{b} \quad (3.17)$$

$\mathbf{u} \times \mathbf{b}$ is the so-called electromotive force. The decomposition (3.13b) implies that the first term of the electromotive force having a nonzero average is $\mathbf{u} \times \mathbf{b}^{(1)}$. However, the solvability condition (3.16a) requires that this term have a curl which has zero average.

Equation (3.14a) determines $\tilde{\mathbf{b}}^{(0)}$ in terms of $\langle \mathbf{b}^{(0)} \rangle$ and the velocity field. In general the solvability condition (3.16a) will not be satisfied, indicating that our choice of scaling is inconsistent. There is, however, one instance when solvability is guaranteed, namely when the velocity field is *parity-invariant*. This means that the velocity field is invariant under $\mathbf{x} \rightarrow -\mathbf{x}$ and $\mathbf{u} \rightarrow -\mathbf{u}$ (fast variables only!). Note that parity-invariance is a broader concept than non-vanishing helicity: the former implies the latter but not conversely. We now show that this implies the vanishing of the mean electromotive force. For a *prescribed* $\langle \mathbf{b}^{(0)} \rangle$, as we perform a parity transform on \mathbf{u} the equation (3.14a) remains intact (because both \mathbf{u} and $\nabla_{\mathbf{x}}$ change sign). Thus $\tilde{\mathbf{b}}^{(0)}$ does not change. Therefore any product of components of \mathbf{u} and $\tilde{\mathbf{b}}^{(0)}$ changes sign. This implies the vanishing of the average of $\mathbf{u} \times \tilde{\mathbf{b}}^{(0)}$.

Equation (3.16b) is closed once $\mathbf{b}^{(1)}$ is determined. The procedure for determining $\mathbf{b}^{(1)}$ is as follows:

- Since $\langle \mathbf{b}^{(0)} \rangle$ is independent of both \mathbf{x} and t the integration of (3.14a) can be effected as if $\langle \mathbf{b}^{(0)} \rangle$ were a constant vector. Furthermore, since $\mathbf{b}^{(1)}$ is linear in $\langle \mathbf{b}^{(0)} \rangle$, the solution for $\mathbf{b}^{(1)}$ will be proportional to $\langle \mathbf{b}^{(0)} \rangle$: $b_i^{(1)} = C_{ij}(\mathbf{x}, t) \langle b_j^{(0)} \rangle$.
- The solution for $\tilde{\mathbf{b}}^{(0)}$ can then inserted in equation (3.14b) to determine $\mathbf{b}^{(1)}$. Since (3.14b) is linear in $\nabla_{\mathbf{x}} \mathbf{b}^{(0)}$, its solution $\mathbf{b}^{(1)}$ will once again be proportional to slow space derivatives of $\mathbf{b}^{(0)}$. Thus we have $b_i^{(1)} = \Gamma_{ijk}(\mathbf{x}, t) \partial_{X_j} \langle b_k^{(0)} \rangle$.
- Inserting $\mathbf{b}^{(1)}$ into the second solvability condition (3.16b) yields a closed equation involving slow second order space derivatives of $\langle \mathbf{b}^{(0)} \rangle$.

In the isotropic case, the resulting equation has the form

$$\partial_T \langle \mathbf{b}^{(0)} \rangle = (\beta + \lambda) \nabla_{\mathbf{x}}^2 \langle \mathbf{b}^{(0)} \rangle. \quad (3.18)$$

(where β is the magnetic analogue of the scalar eddy diffusivity). Contrary to the scalar case the eddy diffusivity $\beta + \lambda$ need not be positive and can drive instabilities.

Next, we consider the transport of a magnetic field when the flow *lacks parity*. This will lead to a new form of the large scale equation demonstrating the so called α -effect. We derive the corresponding equation by a variant of our multiscale formalism, distributing the ϵ 's somewhat differently. We now suspect that there may be large scale effects on shorter $O(\epsilon)$ time scales, so we try

$$\partial_t \leftarrow \partial_t + \epsilon \partial_T$$

$$\partial_{\mathbf{x}} \leftarrow \partial_{\mathbf{x}} + \epsilon \partial_{\mathbf{X}}.$$

Equation (3.12a) becomes

$$(\partial_t + \epsilon \partial_T) \mathbf{b} + \mathbf{u} \cdot (\nabla_{\mathbf{x}} + \epsilon \nabla_{\mathbf{X}}) \mathbf{b} - \mathbf{b} \cdot (\nabla_{\mathbf{x}} + \epsilon \nabla_{\mathbf{X}}) \mathbf{u} = \lambda (\nabla_{\mathbf{x}} + \epsilon \nabla_{\mathbf{X}})^2 \mathbf{b} \quad (3.19)$$

The corresponding hierarchy is

$$O(\epsilon^0): \quad \underline{\partial_t \tilde{\mathbf{b}}^{(0)}} + \underline{\mathbf{u} \cdot \nabla_{\mathbf{x}} \tilde{\mathbf{b}}^{(0)}} - \underline{\mathbf{b}^{(0)} \cdot \nabla_{\mathbf{x}} \mathbf{u}} = \underline{\langle \mathbf{b}^{(0)} \rangle \cdot \nabla_{\mathbf{x}} \mathbf{u}} + \lambda \nabla_{\mathbf{x}}^2 \tilde{\mathbf{b}}^{(0)} \quad (3.20a)$$

$$O(\epsilon): \quad \underline{\partial_t \mathbf{b}^{(1)}} + \underline{\partial_T \tilde{\mathbf{b}}^{(0)}} + \underline{\partial_T \langle \mathbf{b}^{(0)} \rangle} + \underline{\mathbf{u} \cdot \nabla_{\mathbf{x}} \langle \mathbf{b}^{(0)} \rangle} + \underline{\mathbf{u} \cdot \nabla_{\mathbf{X}} \tilde{\mathbf{b}}^{(0)}} + \underline{\mathbf{u} \cdot \nabla_{\mathbf{x}} \mathbf{b}^{(1)}} = \\ \underline{\mathbf{b}^{(1)} \cdot \nabla_{\mathbf{x}} \mathbf{u}} + \underline{\lambda \nabla_{\mathbf{x}}^2 \mathbf{b}^{(1)}} + \underline{2\lambda \nabla_{\mathbf{x}}^2 \tilde{\mathbf{b}}^{(0)}}. \quad (3.20b)$$

As with the previous cases, the underlined terms have zero fast variable average. From (3.20b) the solvability condition is given by

$$\partial_T \langle \mathbf{b}^{(0)} \rangle = \nabla_{\mathbf{x}} \times \langle \mathbf{u} \times \tilde{\mathbf{b}}^{(0)} \rangle. \quad (3.21)$$

However from (3.20a), $\tilde{\mathbf{b}}^{(0)}$ is linear in $\langle \mathbf{b}^{(0)} \rangle$, and thus the mean electromotive force $\langle \mathbf{u} \times \tilde{\mathbf{b}}^{(0)} \rangle$ will be proportional to the mean magnetic field $\langle \mathbf{b}^{(0)} \rangle$:

$$\langle \mathbf{u} \times \tilde{\mathbf{b}}^{(0)} \rangle_i = \alpha_{ij} \langle \mathbf{b}^{(0)} \rangle_j. \quad (3.22)$$

In the isotropic case, $\alpha_{ij} = \alpha \delta_{ij}$, and (2.10) becomes

$$\partial_T \langle \mathbf{b}^{(0)} \rangle = \alpha \nabla_{\mathbf{x}} \times \langle \mathbf{b}^{(0)} \rangle. \quad (3.23)$$

Applying a spatial Fourier transform to (3.23) gives

$$\partial_T \langle \hat{\mathbf{b}}^{(0)} \rangle = i \alpha \mathbf{k} \times \langle \hat{\mathbf{b}}^{(0)} \rangle. \quad (3.24)$$

Seeking eigensolutions in the form $\langle \hat{\mathbf{b}}^{(0)} \rangle = \mathbf{C} e^{\xi t}$ gives $\xi_1 = 0$ and $\xi_{2,3} = \pm k\alpha$. Thus the small-scale structures produce an instability in the mean magnetic field with growth rate proportional to wave number. This is what is usually referred to as the α -effect.

Various remarks can be made.

- Inclusion in the α -effect equation (3.23) of an additional diffusion term can be achieved by modification of the assumed scaling for the molecular diffusivity: instead of an $O(1)$ diffusivity, we take an $O(\epsilon^{-1})$ diffusivity. In the isotropic case, we then obtain:

$$\partial_T \langle \mathbf{b}^{(0)} \rangle = \alpha \nabla_{\mathbf{x}} \times \langle \mathbf{b}^{(0)} \rangle + \lambda \nabla_{\mathbf{x}}^2 \langle \mathbf{b}^{(0)} \rangle. \quad (3.25)$$

The corresponding eigenvalues of (3.25) are $\xi_1 = -\lambda k^2$ and $\xi_{2,3} = \pm \alpha k - \lambda k^2$. Therefore, if $\alpha k - \lambda k^2 > 0$, an amplification in $\langle b^{(0)} \rangle$ is still possible provided the wavenumber k is sufficiently small to render diffusion ineffective.

- b) The form of the equations (3.23) and (3.25) can be guessed by Landau-type symmetry arguments. Performing a Reynolds decomposition of the induction equation (3.12a) gives a “mean” equation

$$\partial_t \mathbf{B} = \nabla_X \times \langle \mathbf{u} \times \mathbf{b}' \rangle + \lambda \nabla_X^2 \mathbf{B}, \quad (3.26)$$

where $\mathbf{B} = \langle \mathbf{b} \rangle$ and $\mathbf{b}' = \mathbf{B} - \langle \mathbf{b} \rangle$ (analogous to, respectively, $\mathbf{b}^{(0)}$ and fluctuating field above). Expanding $\langle \mathbf{u} \times \mathbf{b}' \rangle$ in a Taylor series in slow gradients acting on the mean field gives:

$$\langle \mathbf{u} \times \mathbf{b}' \rangle_i = \alpha_{ij} \mathbf{B}_j + \Gamma_{ijk} \partial_{X_k} \mathbf{B}_k + O(\nabla_X^2 \mathbf{B}). \quad (3.27)$$

Parity invariance of \mathbf{u} implies $\alpha_{ij} = 0$. But, for flows which do not possess parity, α_{ij} need not be zero and, to leading order, we recover (3.22).

- c) A variant of the technique discussed herein can be applied to the question of viscoelasticity of turbulence [6]. When flows possess Galilean invariance, it may be shown that, to leading order, the large scale dynamics are governed by a wave equation involving second order time and space derivatives.

3. CONCLUSIONS

We have shown here how multiscale expansions can be used to systematically analyze the large scale dynamics of scalars and vectors, passively advected by a prescribed small scale flow. For the scalar case, we find that the large scale behavior is always diffusive. The value of the eddy diffusivity (or the eddy diffusivity tensor in the anisotropic case) cannot usually be obtained in closed form; an auxiliary problem, involving only the small scales, must be solved. For the vector case (here a passive magnetic field), the large scale behavior will be superficially diffusive if *parity-invariance* holds. By “superficially”, we mean that it is governed by an equation involving second order space derivatives, but without guarantee that the eddy diffusivity is positive. For flows lacking parity-invariance, the large scale magnetic field will usually be subject to a destabilizing α -effect involving first order space derivatives.

We finally want to stress that essentially the same multiscale analysis which we have applied to the large scale dynamics of a passively advected magnetic field can also be

applied to the problem of the *eddy-viscosity* of a small scale flow \mathbf{u} subject to a weak large scale perturbation \mathbf{w} . The governing equation is the linearized Navier-Stokes equation:

$$\partial_t \mathbf{w} + \mathbf{u} \cdot \nabla_{\mathbf{z}} \mathbf{w} + \mathbf{w} \cdot \nabla_{\mathbf{z}} \mathbf{u} = -\nabla p' + \nu \nabla_{\mathbf{z}}^2 \mathbf{w} \quad (3.28a)$$

$$\nabla_{\mathbf{z}} \cdot \mathbf{u} = 0, \quad \nabla_{\mathbf{z}} \cdot \mathbf{w} = 0. \quad (3.28b)$$

It is clear that its structure is very similar to that of (3.12a,b). The result for large scale velocity perturbations are essentially the same as above: with parity-invariance, we get superficially diffusive behavior, but the eddy viscosity may be negative; without parity-invariance, a new type of instability may be present, the AKA-effect. This is discussed in the next lecture.

Appendix

The demonstration that $\langle \bar{\Theta}^{(0)} \rangle^2 \rightarrow 0$ as $t \rightarrow \infty$ is given here.

Since $\bar{\Theta}^{(0)}$ is ℓ -periodic in \mathbf{z} , it admits a Fourier series representation ($\mathbf{k} = (k_1, k_2, k_3)$)

$$\sum_{\mathbf{k}} \hat{\Theta}_{\mathbf{k}}^{(0)} e^{2i\pi \mathbf{k} \cdot \mathbf{z}/\ell}. \quad (A3.1)$$

The $\mathbf{k} = 0$ coefficient is absent (since $\bar{\theta}$ has zero average); thus, we have the inequality:

$$\sum_{\mathbf{k}} k^2 |\hat{\Theta}_{\mathbf{k}}^{(0)}|^2 \geq \sum_{\mathbf{k}} |\hat{\Theta}_{\mathbf{k}}^{(0)}|^2. \quad (A3.2)$$

Furthermore, invoking Parsevals identity $\langle (\bar{\Theta}^{(0)})^2 \rangle = \sum_{\mathbf{k}} |\hat{\Theta}_{\mathbf{k}}^{(0)}|^2$ and $\langle (\nabla_{\mathbf{z}} \bar{\Theta}^{(0)})^2 \rangle = \sum_{\mathbf{k}} (2\pi k/\ell)^2 |\hat{\Theta}_{\mathbf{k}}^{(0)}|^2$, we obtain the following “Poincaré inequality”:

$$\langle (\nabla_{\mathbf{z}} \bar{\Theta}^{(0)})^2 \rangle \geq (2\pi/\ell)^2 \langle (\bar{\Theta}^{(0)})^2 \rangle. \quad (A3.3)$$

Multiplying the scalar diffusion equation by $\bar{\Theta}^{(0)}$, taking the average over a cell and integrating by parts gives:

$$\frac{1}{2} \partial_t \langle (\bar{\Theta}^{(0)})^2 \rangle \leq -\kappa (2\pi/\ell)^2 \langle (\bar{\Theta}^{(0)})^2 \rangle, \quad (A3.4)$$

so that

$$\langle (\bar{\Theta}^{(0)})^2 \rangle \leq C \exp(-2\kappa(2\pi/\ell)^2 t) \rightarrow 0 \quad \text{as } t \rightarrow \infty. \quad (A3.5)$$

References:

- [1] Papanicolaou, G., Pironneau, O., "On the asymptotic behavior of motions in random flows", Stochastic Nonlinear Systems, Springer, 1981.
- [2] Moffatt, H.K., "Magnetic Field Generation in Electrically Conducting Fluid", Cambridge Univ. Press, 1978.
- [3] Zeldovich, Ya. B., Ruzmaikin, A.A., Sokoloff, D.D., "Magnetic Fields in Astrophysics", Gordon and Breach, 1983.
- [4] Aref, H., J. Fluid Mech., **143**, 1, 1984.
- [5] Dombre, T., Frisch, U., Greene, J.M., Hénon, M., Mehr, A., and Soward, A.M., J. Fluid Mech., **167**, 353, 1986.
- [6] Frisch, U., She, Z.S., and Thual, O., J. Fluid Mech., **168**, 221, 1986.

Frisch #4

**LARGE-SCALE INSTABILITY IN 3-D FLOWS
LACKING PARITY-INVARiance**

Lecture 4:

Uriel Frisch

Notes by S. Roy and A. Leonard

The present notes are meant to supplement material presented in the appended paper by Frisch, She, and Sulem ("Large scale flow driven by the Anisotropic Kinetic Alpha effect", Physica, **28D**, 382, 1987), which will be referred to as FSS. To avoid duplication we do not include a separate reference list.

The α -effect, a large-scale MHD instability, has been known for about 20 years and is usually associated with the presence of helicity. An analogue to the α -effect is known in ordinary fluid dynamics for compressible flows, but was only noticed recently for incompressible three-dimensional, anisotropic flow. As we shall see, a new kind of large-scale instability may exist for incompressible, three-dimensional, anisotropic flows which lack parity-invariance (invariance under simultaneous reversal of position and velocity vectors).

This Anisotropic Kinetic Alpha (AKA) effect can be derived by a small Reynolds number expansion using a separation of scales. The full formal expansion requires six levels of expansion and will not be presented here (see the appendix of FSS).

A small-scale flow, $\mathbf{u}^0(\mathbf{r}, t)$ is driven by a force, $\mathbf{f}(\mathbf{r}, t)$ which is space- and time-periodic. The flow has characteristic length, time, and velocity scales l_0 , t_0 , and V_0 , a small scale Reynolds number, $R = l_0 V_0 / \nu$, and obeys the Navier-Stokes equations (incompressibility conditions are henceforth omitted for brevity)

$$\frac{\partial u_i^0}{\partial t} + \frac{\partial}{\partial x_j} (u_i^0 u_j^0) = - \frac{\partial p^0}{\partial x_i} + \nu \nabla^2 u_i^0 + f_i. \quad (4.1)$$

The basic flow is perturbed to a flow \mathbf{u} having a non-trivial large-scale component

$$\mathbf{u} = \mathbf{w} + \bar{\mathbf{u}}, \quad (4.2)$$

where $\langle \mathbf{u} \rangle = \mathbf{w}$ and the angular brackets denote averaging over the small scales. \mathbf{w} has scales $L \gg l_0$ and $T \gg t_0$ and may be considered as constant over the small scales l_0 and t_0 . The small-scale flow, $\bar{\mathbf{u}}$, is advected by the large-scale flow

$$\frac{\partial \bar{u}_i}{\partial t} + w_j \frac{\partial \bar{u}_i}{\partial x_j} + \frac{\partial}{\partial x_j} (\bar{u}_i \bar{u}_j) = - \frac{\partial \bar{p}}{\partial x_i} + \nu \nabla^2 \bar{u}_i + f_i. \quad (4.3)$$

Therefore, the average small-scale Reynolds stresses,

$$R_{ij} = \langle \bar{u}_i \bar{u}_j \rangle \quad (4.4)$$

will develop a dependence on the mean field and contribute to the large-scale dynamics. The equation for the large-scale velocity components can be derived by introducing slow variables, expanding in Reynolds number, and using the separation of scales to give

$$\frac{\partial w_i}{\partial t} + \frac{\partial}{\partial x_j} (w_i w_j + R_{ij}) = -\frac{\partial p}{\partial x_i} + \nu \nabla^2 w_i. \quad (4.5)$$

This equation is in terms of the slow variables.

The linear regime may be considered when the mean field is weak. The average Reynolds stresses can be expanded in powers of w

$$R_{ij} = \langle u_i^0 u_j^0 \rangle + w_l \left[\frac{\partial \langle \bar{u}_i \bar{u}_j \rangle}{\partial w_l} \right]_{w_l=0}. \quad (4.6)$$

The large scale flow satisfies

$$\frac{\partial w_i}{\partial t} = \alpha_{ijk} \frac{\partial w_k}{\partial x_j} - \frac{\partial p}{\partial x_i} + \nu \nabla^2 w_i, \quad (4.7)$$

with

$$\alpha_{ijk} = - \left[\frac{\partial \langle \bar{u}_i \bar{u}_j \rangle}{\partial w_k} \right]_{w_k=0}. \quad (4.8)$$

The tensor α_{ijk} will vanish for many situations including parity-invariance, isotropy, and a random flow that is δ -correlated in time. The AKA effect vanishes with isotropy because α_{ijk} is symmetric in i and j and there are no non-vanishing isotropic third-order symmetric tensors. The only known instance when α vanishes in both MHD and hydrodynamics is when parity-invariance holds. The AKA effect had not been seen before because assumptions used to derive the equation, made for convenience and not for necessity, caused the effect to disappear. Many closure methods assuming isotropy or δ -correlated in time miss the AKA effect, but the full DIA method of R. Kraichnan should show it. We shall here derive it by multiscale techniques without resort to closure.

A simple example of a flow that lacks parity-invariance and demonstrates the AKA effect by avoiding the known pitfalls is obtained using the following force lacking parity-invariance.

$$\begin{aligned} f_1 &= \frac{\nu V_0 \sqrt{2}}{l_0^2} \cos \left(\frac{y}{l_0} + \frac{\nu t}{l_0^2} \right) \\ f_2 &= \frac{\nu V_0 \sqrt{2}}{l_0^2} \cos \left(\frac{x}{l_0} - \frac{\nu t}{l_0^2} \right) \\ f_3 &= f_1 + f_2. \end{aligned} \quad (4.9)$$

The basic flow is obtained from the linearized Navier-Stokes equations (to leading order in the Reynolds number)

$$\begin{aligned} u_1^0 &= V_0 \cos \left(\frac{y}{l_0} + \frac{\nu t}{l_0^2} - \frac{\pi}{4} \right) \\ u_2^0 &= V_0 \cos \left(\frac{x}{l_0} - \frac{\nu t}{l_0^2} + \frac{\pi}{4} \right) \\ u_3^0 &= u_1^0 + u_2^0. \end{aligned} \quad (4.10)$$

For low Reynolds numbers of the basic flow (as we henceforth assume), the small-scale flow is essentially a Stokes flow with forcing and advection by the large-scale (quasi-uniform) flow \mathbf{w} ; it thus satisfies the following equation (to leading order)

$$\frac{\partial \bar{u}_i}{\partial t} + w_j \frac{\partial \bar{u}_i}{\partial x_j} = \nu \nabla^2 \bar{u}_i + f_i. \quad (4.11)$$

This can be solved with Fourier transforms or a Galilean transformation to calculate the average small-scale Reynolds stresses.

$$\begin{aligned} R_{11} &= R_{13} = \frac{V_0^2}{2} - \frac{V_0^2 l_0 w_2}{2\nu} + O(w^2) \\ R_{22} &= R_{23} = \frac{V_0^2}{2} + \frac{V_0^2 l_0 w_1}{2\nu} + O(w^2) \\ R_{33} &= R_{11} + R_{22} \\ R_{12} &= 0. \end{aligned} \quad (4.12)$$

The non-vanishing components of α_{ijk} for the linear AKA effect are therefore

$$\alpha_{112} = \alpha_{132} = \alpha_{332} = -\alpha_{221} = -\alpha_{231} = -\alpha_{321} = -\alpha_{331} = \alpha = \frac{V_0^2 l_0}{2\nu}. \quad (4.13)$$

The equation for the large-scale motion can be solved now that R_{ij} is known. The most unstable modes depend only on z , so large-scale perturbations depending only on z satisfy

$$\frac{\partial w_1}{\partial t} = \alpha \frac{\partial w_2}{\partial z} + \nu \frac{\partial^2 w_1}{\partial z^2} \quad (4.14)$$

$$\frac{\partial w_2}{\partial t} = -\alpha \frac{\partial w_1}{\partial z} + \nu \frac{\partial^2 w_2}{\partial z^2}. \quad (4.15)$$

The solution is of the form

$$\psi = w_1 + i w_2 = e^{ikz} e^{(\alpha k - \nu k^2)t}, \quad (4.16)$$

so that wavenumbers satisfying $kl_0 < \frac{R^2}{2}$ are unstable.

The scale of the instability increases as the Reynolds number decreases. The large-scale flow that results from this instability is a helical standing wave, with circular polarization and exponentially growing amplitude. This is an example of a Beltrami flow.

Numerical experiments were performed to confirm the AKA effect. Pseudo-spectral simulations with 32^3 points used forcing at $k = 6$ and $R = \sqrt{1/2}$, the only linearly unstable mode being $k = 1$. At such moderately small Reynolds numbers, subleading order effects are significant (about 40 percent) but the qualitative picture is present. Note that much smaller Reynolds number calculations require very fine resolution to get a separation of scales. The resolution goes up as R^{-2} and the computational effort rises as R^{-8} . The linear AKA effect is clearly seen from the numerical simulation results in Figure 4.1 for times up to about $t = 3.5$. The small initial energy in the $k = 1$ mode decays at first, because stable and unstable modes are competing. The exponential growth (Beltrami runaway) then takes over until the large scales have enough energy that the linear equations are no longer valid.

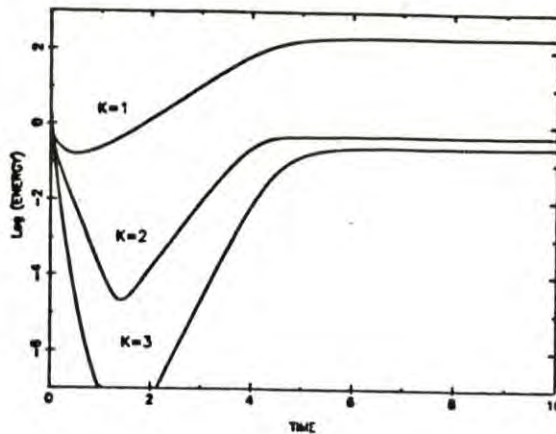


Figure 4.1: Full numerical simulation of 3-D Navier Stokes equation showing AKA instability and saturation. After FSS.

Beyond $t = 3.5$ we observe saturation. Physically, this is due to the feed-back effect of the large-scale flow. Against a strong background flow it becomes more difficult for the prescribed force to produce small-scale flow. Thus the small-scale Reynolds stresses should be decreasing. Indeed, when we solve eq. (4.3), ignoring the nonlinear term $\partial(\bar{u}_i \bar{u}_j)/\partial x_j$,

(which is irrelevant at low Reynolds number), we find that the Reynolds stresses have a nonlinear dependence on the mean flow w , with a w^{-2} behavior for large w 's. The nonlinear equation for the large-scale dynamics incorporating the correct Reynolds stresses (in their full nonlinear dependence) are given below in nondimensional form:

$$\begin{aligned} \frac{\partial w_1}{\partial t} + \frac{1}{2} \frac{\partial}{\partial z} \left[\frac{1}{1 + R w_2 + \frac{1}{2}(R w_2)^2} \right] &= \frac{1}{R} \frac{\partial^2}{\partial z^2} w_1 \\ \frac{\partial w_2}{\partial t} + \frac{1}{2} \frac{\partial}{\partial z} \left[\frac{1}{1 - R w_1 + \frac{1}{2}(R w_1)^2} \right] &= \frac{1}{R} \frac{\partial^2}{\partial z^2} w_2, \end{aligned} \quad (4.17)$$

where $R = V_0 l_0 / \nu$. Here the length scale is l_0 and the velocity scale is V_0 . A naive dimensional analysis of these equations suggests that, in the nonlinear regime, the amplitudes of the w 's should be $O(R^{-1})$, their spatial scale $O(R^{-2})$, and their temporal scale $O(R^{-3})$. Thus, for small R , we expect very strong fields to form eventually on very large scales.

We now report some recent results of Frisch, Scholl, She and Sulem concerning the possibility of an inverse cascade ("A new large-scale instability in three-dimensional anisotropic incompressible flows lacking parity-invariance" Proc. IUTAM Symposium on Fundamental Aspects of Vortex Motion, Tokyo, Sept. 1987) It is known that the α -effect in MHD is the main motor of the "inverse helicity cascade" (see D. Montgomery's lectures). Could it be that in ordinary incompressible 3-D flows there is an inverse cascade driven by the AKA-effect? The possibility of an inverse cascade of helicity was considered already by Brissaud et. al. (1973, Phys. Fluids 16, 1366). Later, André and Lesieur (J. Fluid Mech. 81, 187, 1977) showed that within an isotropic closure framework the possibility is ruled out. However, the AKA-effect is inherently anisotropic, so the question is worth reexamining.

We assume that there is a whole range of linearly unstable wavenumbers below the cutoff wavenumber $k_* = R^2/(2l_0)$ for linear stability. If there is an inverse cascade we expect to see with increasing time the peak of excitation to migrate to lower and lower wave numbers, while becoming increasingly strong. Such a cascade cannot just follow from linear growth of unstable modes, since they would forever give dominance of the most unstable mode. For the AKA-effect the linear growth rate is $\alpha k - \nu k^2$, and the most unstable mode is $k = k_*/2$. A necessary condition for the establishment of an inverse cascade is that the linearly unstable mode with the smallest non-vanishing k should eventually dominate, in spite of its lower linear growth rate.

A first numerical experiments was set up, looking for such evidence. It had modes $k = 1$ through 4 unstable, with maximum growth rate at $k = 2$. The results are shown

in figure 4.2, where only modes 1, 2 and 9 are shown for clarity. Up to about $t = 0.5$ we obtain the exponential growth in which mode 2 is growing much faster than mode 1, as predicted by the linear theory. After that time, nonlinear effects become significant and at about $t = 0.6$ we observe a kind of saturation reminiscent of what we saw when there was only a single linearly unstable mode. This is however just a plateau from which the system quickly escapes. The most salient feature is that mode $k = 1$ "leap-frogs" mode $k = 2$ around $t = 0.9$. Eventually the system goes to an approximately steady state in which mode $k = 1$ significantly dominates over mode $k = 2$.

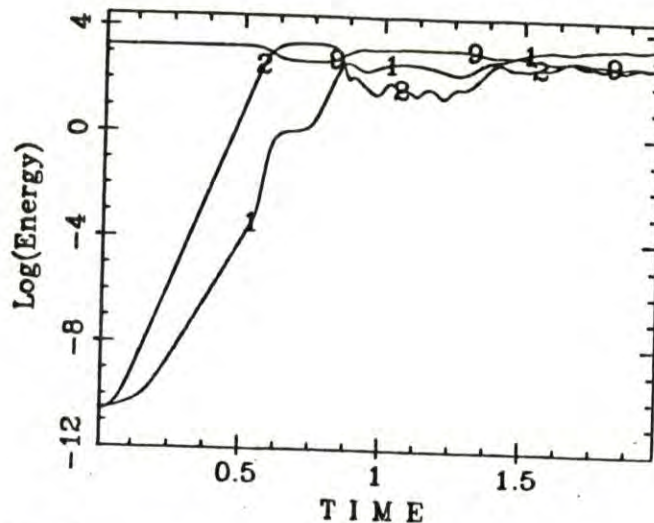


Figure 4.2: AKA instability with two linearly unstable modes ($k = 1$ and $k = 2$). Mode $k = 2$ is the linearly fastest growing, but eventually mode $k = 1$ "leap-frogs" it, an indication that we may see the beginning of an inverse cascade. After Frisch, Scholl, She, and Sulem (1987).

We stress that we have not yet seen direct evidence for an inverse cascade, but just one necessary symptom. Experiments using much higher resolution and very considerable computational resources are needed to confirm the existence of an inverse cascade.

Note added in proof. Numerical integration and theoretical analysis of the set of nonlinear PDE's (4.17) have demonstrated the existence of the inverse cascade. Cases have been studied with up to 300 linearly unstable modes (Sulem, She, Scholl, and Frisch, "Generation

of large-scale structures in three-dimensional flows lacking parity-invariance", submitted to J. Fluid Mech., 1988)

Frisch#5

LATTICE GAS HYDRODYNAMICS: INTRODUCTION

These lecture notes, written by the participants of the summer school, should be considered as supplementing the paper "Lattice gas hydrodynamics in two and three dimensions" by Frisch, d'Humières, Hasslacher, Lallemand, Pomeau, and Rivet (*Complex Systems*, 1, 648, 1987), which has been appended to these lecture notes. All literature citation is to the reference list at the end of this paper, denoted hereafter FDHLPR.

1. INTRODUCTION

A novel technique that has recently been applied to the study of hydrodynamics is that of Cellular Automata (CA). CA's are discrete states attached to the nodes of a regular lattice with an updating rule involving only a small number of neighbours. Figures 5.1, 5.2, and 5.3 illustrate well-known fluid mechanical problems that have been simulated using this technique. Figure 5.1 shows a snapshot of a two-dimensional Karman vortex street behind a flat plate; it is taken from Ref. 31. Figure 5.21 shows a snapshot of the recent three-dimensional lattice gas calculations behind a circular plate, as performed by J.-P. Rivet (Rivet, Hénon, Frisch, and d'Humières, submitted to *Europhys. Lett.*, 1988). Figure 5.3 shows the evolution of a Rayleigh-Taylor instability (Ref. 57). For historical perspective on CA's and their lattice gas version, the reader is referred to Sec. 1 of FDHLPR.

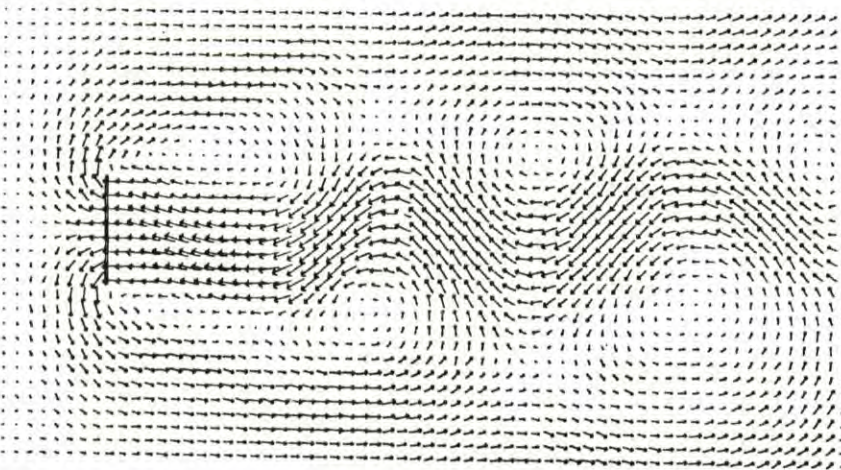


Figure 5.1: Karman vortex street behind a flat plate simulated on FPS 164 at Ecole Normale Supérieure. From d'Humières, Pomeau, and Lallemand (1985). (Ref. 26)

Lecture 5:

U. Frisch

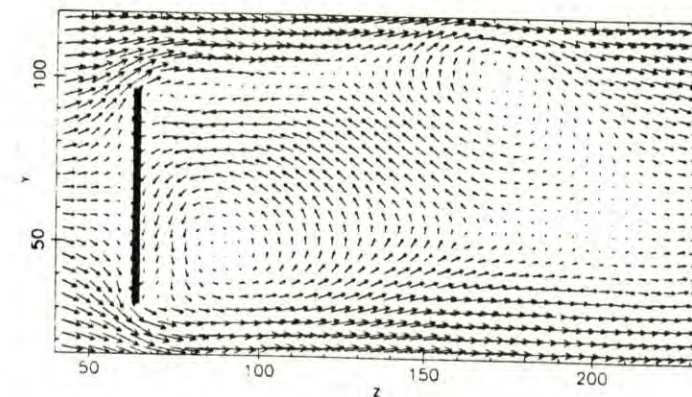


Figure 5.2: A snapshot of the recent three-dimensional lattice gas calculation of flow behind a circular plate, from Rivet et al. (1988). Shown, is a detail of an axial cut of the velocity field. Note that the axial symmetry is broken.

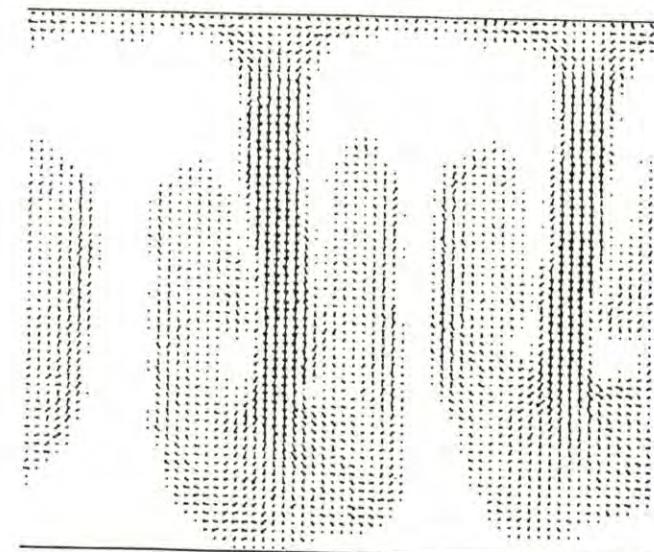


Figure 5.3: Rayleigh-Taylor instability simulated by Clavin, Lallemand, Pomeau, and Searby (1987). (Ref. 57).

There are many precedents in physics of simple, discrete models able to correctly capture complexities of the real world. A prominent example is the Ising model, which is a very poor substitute for the intricate atomic interactions in a ferromagnet, but still manages to capture the essence of critical phase transitions. This is indeed revealed by the Renormalization Group analysis (fully exploiting the physical idea of spin-blocking), which demonstrates that the real world and the Ising model differ only in "irrelevant" details.

Similarly, there are many models leading to fluid dynamics. Traditionally, turbulence theories have attempted to model phenomena through statistical averages of the velocity field. This field is however itself an average over microscopic motion. Is it conceivable that something can be gained by "undoing" such averages, reverting either to the full microscopic world (molecular dynamics), or to artificial, discrete CA models emulating the former in its macroscopic consequences? First, we must try to understand what the key ingredients are which lead from the microscopic laws of motion to fluid dynamics. In the real world, equilibria are parametrized by three thermodynamic quantities: the density ρ , the fluid velocity u , and the temperature T , associated with the conservation of mass, momentum, and energy, respectively. The fluid dynamical equations are obtained by patching together "local" equilibria, changing slowly in space and time. It was already stressed by Maxwell that the details of the intermolecular forces are unimportant in deriving his celebrated law for the velocity distribution and the fluid dynamical equations. Such details only affect the values of the transport coefficients. In addition to the conservation laws, basic symmetries of Newtonian physics seem to play a crucial role in determining the form of the fluid dynamical equations. These include:

- continuous spatio-temporal translations,
- arbitrary 3-D rotations,
- time reversal,
- space reversal (parity),
- Galilean transformations.

For example, the latter essentially provides a unique determination of the nonlinear term $u \cdot \nabla u$. If we were to insist on keeping all these symmetries, there is little we could do, short of staying in the real world. The key question is to see whether *discrete* models can be constructed in which one or more of these invariance properties are by necessity relaxed without losing fluid dynamical behaviour. Certainly, discrete translational invariance in space and time does not preclude continuous invariances on large scales. Less obvious is that

discrete rotations will not violate the requirement of isotropy. Even less obvious is the fact that Galilean invariance is not violated macroscopically. These issues will be addressed in forthcoming lectures.

Finally, it may be asked why we insist on making discrete CA models. The fact that the Ising model has played an essential role in the understanding of ferromagnetics was certainly one of the original motivations of Hardy, Pomeau, and de Pazzis when they introduced the first lattice gas model in the early seventies (Refs. 22-24). For computational implementation, discrete models are appealing in view of the Boolean structure of computers. One of the most promising trends in computer architecture is towards parallelism and even *massive* parallelism. In the latter, the number of concurrent processors can, in principle, grow indefinitely, as is the case when processors interact only with nearest neighbours. This provides additional reasons to explore the possibilities of CA models of fluid dynamics.

Frisch #6

LATTICE GAS HYDRODYNAMICS: MICRODYNAMICS

Notes by L. M. Polvani and S. Derbyshire

The Navier-Stokes equations are themselves isotropic, and it is important that a lattice-gas model preserve this property. Specifically, we hope to recover at the macroscopic level an equation of the form:

$$\partial_t(\rho u)_\alpha + \partial_\beta(P_{\alpha\beta}) = \text{viscous terms}, \quad (6.1)$$

where the symmetrical momentum flux tensor is:

$$P_{\alpha\beta} = p\delta_{\alpha\beta} + \rho u_\alpha u_\beta. \quad (6.2)$$

The most general parity-invariant form for $P_{\alpha\beta}$ up to second-order in u (one may think of this as a Taylor-series for the limit when flow speeds are much less than particle speeds) is:

$$P_{\alpha\beta} = (T_{\alpha\beta}^0 + T_{\alpha\beta\gamma\delta}u_\gamma u_\delta). \quad (6.3)$$

In 2-D, assuming $T_{\alpha\beta\gamma\delta}$ to be symmetric pairwise in (α, β) and in (γ, δ) , a sufficient condition for isotropy is that $T_{\alpha\beta\gamma\delta}$ be invariant under $\pi/3$ -rotations (the full proof was given in the lecture - see FDHLPR, sec. 6). This motivates the choice (in 2-D) of the "FHP" lattice, based on equilateral triangles (figure. 3 of FDHLPR).

In 3-D, however, no regular crystal is fully isotropic (the icosahedron is isotropic but cannot be packed). Hence, any attempt to implement lattice-gas dynamics on a regular 3-D grid will lead, in the macroscopic limit, to extra terms inconsistent with the Navier-Stokes equations.

If one excludes random or quasi-lattices, then a four-dimensional representation must be sought. This has led to the introduction of the Face-Centered-Hyper-Cubic lattice (FCHC), defined as:

$$\text{FCHC} = \{(x_1, x_2, x_3, x_4) \in \mathbb{Z}^4 \mid x_1 + x_2 + x_3 + x_4 = 2\sigma \quad (\sigma \in \mathbb{Z})\}. \quad (6.4)$$

The FCHC lattice has the following properties:

1. Any node has 24 nearest-neighbours.
2. FCHC is invariant under coordinate permutations, and reversal of any or several coordinates.

Lecture 6:
U. Frisch

3. FCHC is invariant under the isometry $x_\alpha \rightarrow x_\alpha - \sigma$.
4. It follows from 2 and 3 that the tensor, $T_{\alpha\beta\gamma\delta}$, governing the macroscopic stress-strain relation is isotropic.

In practice, one works with the *pseudo-4-D* model, with a width of only one node in the fourth direction (i.e., formally assuming unit periodicity). Implementation of this lattice leads to the usual Navier-Stokes equations. In macroscopic terms, FCHC conserves density and momentum. The fourth conserved quantity associated with the four-velocity can be shown to behave effectively as a passive scalar in the incompressible limit, and hence induces no spurious dynamical effects.

Having chosen a lattice with the appropriate symmetries, consider now the equations of motion for particles on such a lattice. Each node ('gridpoint') has b cells, where b is the number of bits per node, and a cell is an 'in'- or 'out'-port leading to or from another node. The 'microdynamics' on the lattice is described by a Boolean field, which is the cellular automaton analog of Hamilton's equations of motion in classical statistical mechanics.

Let $n_i(t_*, \mathbf{r}_*)$ be the Boolean field at discrete time t_* and node \mathbf{r}_* (starred quantities being discrete), where 1 denotes 'occupied' and 0 'vacant' for cell i . Let $\mathbf{r}_* + \mathbf{e}_i$ be the set of nearest neighbours of the node \mathbf{r}_* . One may think of the updating rule for the CA at each time-step in two stages: collision and propagation. For instance, in the HPP case (a square, 2-D lattice - see figure. 1 of FDHLPR), the rule is given by:

$$\begin{aligned} n_i(t_* + 1, \mathbf{r}_* + \mathbf{e}_i) = & (n_i \wedge \neg(n_i \wedge n_{i+2} \wedge \neg n_{i+1} \wedge \neg n_{i+3})) \\ & \vee (n_{i+1} \wedge n_{i+3} \wedge \neg n_{i+3} \wedge \neg n_i \wedge \neg n_{i+2}), \end{aligned} \quad (6.5)$$

where \wedge , \vee , \neg are the Boolean symbols for 'and', 'or' and 'not' respectively. This can also be expressed in the arithmetical form:

$$\begin{aligned} n_i(t_* + 1, \mathbf{r}_* + \mathbf{e}_i) = & n_i(t_*, \mathbf{r}_*) + n_{i+1}n_{i+3}(1 - n_i)(1 - n_{i+2}) \\ & - n_i n_{i+2}(1 - n_{i+1})(1 - n_{i+3}), \end{aligned} \quad (6.6)$$

which is reminiscent of the Boltzmann equation.

It is shown in the next lecture how the macrodynamical equations of motion can be derived from the above by taking ensemble averages.

Frisch #7

LATTICE GAS HYDRODYNAMICS: COLLISIONS AND EQUILIBRIA

Lecture 7:

U. Frisch

In order to write the microdynamical equation for less elementary lattices we need to introduce a more compact notation. This notation will allow the use of both probabilistic and deterministic collision rules. In all cases the collision rules must ensure exact conservation laws for mass and momentum. Here is an example of a nondeterministic collision rule. On the triangular FHP lattice, a "head-on" collision with exactly two in-coming particles at 0° and 180° can have two results: out-going particles at either 60° and 240° , or 120° and 300° . If only one of these possibilities is chosen, 'chirality' is introduced into the model, i.e. the model is not invariant under reflection. Similarly, on the FCHC lattice used for the pseudo-4-D model, head-on collisions have 11 possible choices for outgoing channels. An advantage of probabilistic collision rules is that it may eventually make it easier to prove rigorous results, using tools from ergodic theory. Indeed, the possibility of there being several non-communicating cycles of lattice configurations, spoiling ergodicity, is then easily ruled out.

It is useful to make a distinction between random variables and their assignment. When we assign a Boolean variable n_i some value, the assignment will be denoted by s_i . The subscript i runs from 1 to b , where b is the number of neighbors, and thus the number of bits for each site. The HPP lattice has $b = 4$, the FHP lattice has $b = 6$, and the FCHC lattice has $b = 24$. Further, we shall denote the in-state, that before the collision, by $s = \{s_i\}$, and the out-state, that after the collision, by s' . For the deterministic system each s leads to a well-defined s' , while in the probabilistic case transition probabilities are used. Define $A(s \rightarrow s')$ as the probability of going to state s' from state s . We shall also need the Boolean variable

$$\xi_{ss'}, \quad \langle \xi_{ss'} \rangle = A(s \rightarrow s') \quad (7.1)$$

to represent individual realizations of the probabilistic collision process. For a given s there is a unique s' such that $\xi_{ss'} = 1$. At each r_* and t_* a new $\xi_{ss'}$ is chosen with the same statistics.

The conservation laws are expressed by the equations

$$\sum_i (s'_i - s_i) A(s \rightarrow s') a_i = 0, \quad \forall s, s' \quad (7.2)$$

where

$$a_i = \begin{cases} 1 & \text{for all } i \\ c_{i\alpha}, & \alpha = 1, \dots, D \end{cases} \quad (7.3)$$

and D is the spatial dimension of the lattice. The vector c_i connects each node to its nearest neighbor in the i -direction. The case $a_i = 1$ corresponds to mass conservation, while $a_i = c_{i\alpha}$ corresponds to momentum conservation. We also require that there be no other independent set of a_i 's for which the eqs. (7.2) are satisfied, as this would imply the existence of *spurious* conservation laws. One way to detect spurious conservation laws is to use the linearized Boltzmann approximation (FDHLPR, sec. 8.2): the null modes of the linearized collision operator correspond to the individual scalar conservation laws.

The most general microdynamical equation for a lattice gas is

$$n_i(t_* + 1, r_* + c_i) = \sum_{s, s'} s'_i \xi_{ss'} \prod_j n_j^{s_j} (1 - n_j)^{1-s_j}. \quad (7.4)$$

This can be verified by inspection. The product term is the Boolean equivalent of a delta-function; it is zero unless the pattern of s 's matches the pattern of n 's. Thus the only term appearing in the sum over s is the one consistent with the state $n_i(t_*, r_*)$. The $\xi_{ss'}$ gives the out-state, and the s'_i says that the final n_i is the relevant s'_i .

So far, the only non-deterministic element is in ξ . Now, as is usual in statistical mechanics, we introduce an *ensemble* of initial conditions, each with its own probability:

$$P(t = 0, s(\cdot)) \geq 0, \quad \sum_{s(r_*)} P = 1, \quad (7.5)$$

where $s(\cdot) = \{s(r_*)\}$ is a configuration in the set $\Gamma = \{s(\cdot)\}$, the set of all configurations. Probabilities now enter twice: in the choice of initial conditions, and in the non-deterministic collision rules. The equation of evolution for P (the Liouville equation) is

$$P(t_* + 1, Ss'(\cdot)) = \sum_{s(\cdot) \in \Gamma} \prod_{r_*} A(s \rightarrow s') P(t_*, s(\cdot)), \quad (7.6)$$

where the streaming operator S is defined by:

$$S : s_i(r_*) \mapsto s_i(r_* - c_i). \quad (7.7)$$

We can now take averages with respect to this probability distribution. The most useful quantities are the mean populations:

$$N_i(t_*, r_*) = \langle n_i(t_*, r_*) \rangle, \quad \langle (\cdot) \rangle = \sum_{s(\cdot)} (\cdot) P. \quad (7.8)$$

The relevant hydrodynamic quantities, the density per node $\rho(t_*, \mathbf{r}_*)$, and the mass current per node $\mathbf{j}(t_*, \mathbf{r}_*)$, can be constructed from the mean populations:

$$\begin{aligned}\rho(t_*, \mathbf{r}_*) &= \sum_i N_i \\ \mathbf{j}(t_*, \mathbf{r}_*) &= \rho \mathbf{u} = \sum_i \mathbf{c}_i N_i,\end{aligned}\quad (7.9)$$

where \mathbf{u} is the hydrodynamic velocity. Note that, depending on the lattice, the number of nodes per unit volume may be different from one. Eventually we shall want to extract equations for the large-scale behavior of ρ and \mathbf{j} . The latter will be derived from a simple form of the local conservation equations:

$$\begin{aligned}\sum_i N_i(t_* + 1, \mathbf{r}_* + \mathbf{c}_i) &= \sum_i N_i(t_*, \mathbf{r}_*) \\ \sum_i \mathbf{c}_i N_i(t_* + 1, \mathbf{r}_* + \mathbf{c}_i) &= \sum_i \mathbf{c}_i N_i(t_*, \mathbf{r}_*).\end{aligned}\quad (7.10)$$

These equations are exact equations, and they express that at each node the collisions conserve mass and momentum. Since the nodes are not summed over they represent as many conservation relations as there are nodes.

Now that we have a probabilistic formulation, the next step is to look for equilibrium distributions. An equilibrium distribution can be guessed by analogy with ordinary statistical mechanics, and then checked to verify that it is indeed a steady state solution of the Liouville equation. In the real world, the difficulties in finding the equilibrium distribution comes from correlations between particles, which occur due to finite range interactions. Since for the lattice gas the range of interaction is zero, we expect that the equilibrium distribution will factorize into distributions at each site:

$$P(s(\cdot)) = \prod_{\mathbf{r}_*} p(s(\cdot)). \quad (7.11)$$

Of course the equilibrium state must be translation-invariant, so p is independent of \mathbf{r}_* . To choose p we ask what is the most general Boolean distribution at a node? There are b variables at each node, and if they are all independent then

$$p(s(\cdot)) = \prod_i N_i^{s_i} (1 - N_i)^{1-s_i}. \quad (7.12)$$

The next step is to substitute this 'guesstimated' distribution into the Liouville equation to see if it is correct. Since the distribution is translation-invariant we can ignore the

streaming operator S . In addition, we only need to check the distribution at a single node. Now, at each node there are b unknowns, N_i , but there are 2^b equations. It so happens that the above distribution is indeed the equilibrium distribution provided an additional assumption is made: semi-detailed balance. Recall that for any transition probability

$$\sum_{s'} A(s \rightarrow s') = 1, \quad \forall s. \quad (7.13)$$

Semi-detailed balance is the statement that

$$\sum_s A(s \rightarrow s') = 1, \quad \forall s'. \quad (7.14)$$

This holds trivially for one-to-one deterministic collisions. In the non-deterministic case, semi-detailed balance is equivalent to the statement that if there is equal probability of all states before the collision, then there will be equal probability of all states after the collision. A stronger condition, which is unnecessary here, is detailed balance, also called micro-reversibility:

$$A(s \rightarrow s') = A(s' \rightarrow s). \quad (7.15)$$

With the assumption of semi-detailed balance one can prove that the following three statements are equivalent:

- a. The N_i 's are solutions of the 2^b Liouville equations.
- b. The N_i 's are solutions of the b equations

$$\sum_{s,s'} (s'_i - s_i) A(s \rightarrow s') \prod_j N_j^{s'_j} (1 - N_j)^{1-s_j} = 0. \quad (7.16)$$

- c. The N_i 's are given by:

$$N_i = \frac{1}{1 + \exp(h + \mathbf{q} \cdot \mathbf{c}_i)}, \quad h, \mathbf{q} \text{ arbitrary.} \quad (7.17)$$

Although it cannot be proved that this is the only equilibrium distribution, all numerical simulations on decent size lattices ($\sim 16 \times 16$ or larger) show quick relaxation to this distribution. From the above results follows immediately a *universality theorem*: Any lattice gas satisfying semi-detailed balance has universal equilibria with mean populations depending only on density $\rho = \sum_i N_i$, and mass current $\mathbf{j} = \sum_i \mathbf{c}_i N_i$, independent of the detailed collision laws.

Frisch #8

LATTICE GAS HYDRODYNAMICS: FROM MICRODYNAMICS TO THE NAVIER-STOKES EQUATIONS

Notes prepared by M. Hadfield and S. Roy

We have a field of Boolean variables $n_i(t_*, \mathbf{r}_*)$ describing the state of the b links connected to each node on a D -dimensional lattice and a set of velocity vectors \mathbf{c}_i having common modulus c . Averaging over an ensemble of configurations of the field yields the mean populations

$$N_i(t_*, \mathbf{r}_*) = \langle n_i(t_*, \mathbf{r}_*) \rangle, \quad (8.1)$$

and the mean density and mass current

$$\rho(t_*, \mathbf{r}_*) = \sum_i N_i(t_*, \mathbf{r}_*), \quad \rho\mathbf{u} = \sum_i \mathbf{c}_i N_i(t_*, \mathbf{r}_*). \quad (8.2)$$

The conservation relations for mass and momentum are

$$\begin{aligned} \sum_i N_i(t_* + 1, \mathbf{r}_* + 1) &= \sum_i N_i(t_*, \mathbf{r}_*), \\ \sum_i \mathbf{c}_i N_i(t_* + 1, \mathbf{r}_* + 1) &= \sum_i \mathbf{c}_i N_i(t_*, \mathbf{r}_*). \end{aligned} \quad (8.3)$$

Energy conservation has not been introduced separately because it is implied by mass conservation, since all \mathbf{c}_i have the same magnitude. For physical systems where a separate macroscopic energy conservation law must be imposed a multi-speed lattice model can be used. The most common multi-speed models include "rest" particles of zero speed. For example, we can generalise the HPP model to include diagonally traveling particles, with speed $\sqrt{2}$, and rest particles (ref. 2 of FDHLPR). Collision laws may then be defined such that mass, momentum and energy are conserved independently. However, this lattice has insufficient symmetry to converge to the Navier-Stokes equations, so one has to resort to multi-speed variants of the FHP triangular model to obtain a non-trivial energy variable. We shall not pursue the matter further.

The assumption of semi-detailed balance (FDHLPR section 2.4) leads to universal equilibrium solutions with mean populations given by the Fermi-Dirac distribution

$$N_i = f_{FD}(h + \mathbf{q} \cdot \mathbf{c}_i) \quad \text{where} \quad f_{FD}(x) = \frac{1}{1 + e^x}. \quad (8.4)$$

Lecture 8:
U. Frisch

The invariants of the lattice determine the properties of the equilibria, as we shall see below. The Lagrange multipliers, $h(\rho, \mathbf{u})$ and $\mathbf{q}(\rho, \mathbf{u})$, are calculable in principle through the relations

$$\begin{aligned} \rho &= \sum_i f_{FD}(h + \mathbf{q} \cdot \mathbf{c}_i), \\ \rho\mathbf{u} &= \sum_i \mathbf{c}_i f_{FD}(h + \mathbf{q} \cdot \mathbf{c}_i). \end{aligned} \quad (8.5)$$

In general, solutions are not known in closed form. Still, for hydrodynamic velocities small compared to particle velocities, the equilibria can be calculated perturbatively. We expand h and \mathbf{q} in powers of \mathbf{u} , expand the Fermi-Dirac distribution and apply the constraints for average mass and momentum. The derivation is described in FDHLPR section 4.2 and the resulting equilibrium mean populations to second order are

$$N_i^{eq} = \frac{\rho}{b} + \frac{\rho D}{c^2 b} \mathbf{c}_{i\alpha} u_\alpha + \rho G(\rho) Q_{i\alpha\beta} u_\alpha u_\beta + O(u^3),$$

where

$$G(\rho) = \frac{D^2}{2c^4 b} \frac{b - 2\rho}{b - \rho} \quad \text{and} \quad Q_{i\alpha\beta} = \mathbf{c}_{i\alpha} \mathbf{c}_{i\beta} - \frac{c^2}{D} \delta_{\alpha\beta}. \quad (8.6)$$

This is of course just an expansion of N_i in powers of \mathbf{u} . The first two terms in the expansion could have been deduced simply by noting that N_i will have to have some expansion in powers of \mathbf{u} , and requiring that it satisfy the mass and momentum constraints together with the lattice symmetries. However, the quadratic term could not have been found this way; it depends on N_i having a Fermi-Dirac distribution. Some features of that term could still have been guessed. When $Q_{i\alpha\beta}$ is summed over i it must give zero to avoid perturbing the mass constraint. Similarly, when it is multiplied by $\mathbf{c}_{i\alpha}$ and summed over i it must give zero to avoid perturbing the momentum equation.

That $G(\rho) = 0$ when $\rho = b/2$ could also have been guessed. Consider a "duality" transformation which interchanges particles and holes. If the equilibrium is independent of the details of the interaction laws (as is ensured by semi-detailed balance) then $N_i \rightarrow 1 - N_i$ under a duality transformation, and the velocity \mathbf{u} will reverse. When $\rho = b/2$, this implies the vanishing of quadratic terms in the velocity.

The *macrodynamical* equations can now be constructed by glueing together local equilibria of the above form. Assume that ρ and \mathbf{u} are changing on a spatial scale ϵ^{-1} , that density is $O(1)$ and that \mathbf{u} is small compared to the particle speed. We expect the following phenomena

- a. relaxation to local equilibria on a time scale independent of ϵ (say, just a few collision times),
- b. density perturbations propagating as sound waves on time scale ϵ^{-1} , because the velocity of sound will be $O(1)$ and the distance will be $O(\epsilon^{-1})$,
- c. diffusive effects on time scale ϵ^{-2} because the length scale is ϵ^{-1} and the microscopic viscosity is $O(1)$.

If $N_i^{(0)}$ is the mean equilibrium population based on the local ρ and u , then for small ϵ the actual mean population $N_i(t, \mathbf{r})$ may be expanded in powers of ϵ

$$N_i(t, \mathbf{r}) = N_i^{(0)}(t, \mathbf{r}) + \epsilon N_i^{(1)}(t, \mathbf{r}) + O(\epsilon^2), \quad (8.7)$$

where the time and space variables are now treated as continuous. The boolean conservation relations for mass and momentum can now be expanded in powers of ϵ , assuming that ρ and u can be smoothly interpolated to continuous space-time (FDHLPR sec. 5). To leading order, $O(\epsilon)$, the result is a mass continuity equation (FDHLPR eq. 5.6) and an Euler-like momentum equation (FDHLPR eq. 5.7). Care must be taken in deriving the second order approximations to incorporate diffusion effects: all the finite difference must then be expanded to second order.

The *macrodynamical* momentum equation (FDHLPR eq. 5.16) has a strong resemblance to the Navier-Stokes equation, but with the discrete rotational symmetries still entering via a fourth order tensor, $T_{\alpha\beta\gamma\delta}$. For those lattices having suitable symmetries (see the lecture on the crystallographic aspects), the macrodynamical equations can be written, in a form which brings out their similarities with the equations of fluid dynamics, namely

$$\begin{aligned} \partial_t \rho + \partial_\beta (\rho u_\beta) &= 0 \\ \partial_t (\rho u_\alpha) + \partial_\beta P_{\alpha\beta} &= \partial_\beta S_{\alpha\beta} + O(\epsilon u^3) + O(\epsilon^2 u^2) + O(\epsilon^3 u), \end{aligned} \quad (8.8)$$

where the momentum flux tensor $P_{\alpha\beta}$ is

$$P_{\alpha\beta} = c_s^2 \rho \left(1 - g(\rho) \frac{u^2}{c^2} \right) \delta_{\alpha\beta} + \rho g(\rho) u_\alpha u_\beta \quad (8.9)$$

and the viscous stress tensor $S_{\alpha\beta}$ is

$$S_{\alpha\beta} = (\nu_c(\rho) + \nu_p) \left(\partial_\alpha (\rho u_\beta) + \partial_\beta (\rho u_\alpha) - \frac{2}{D} \delta_{\alpha\beta} \partial_\gamma (\rho u_\gamma) \right). \quad (8.10)$$

c_s^2 , ν_p , and $g(\rho)$ are defined as follows (FDHLPR eq. 6.17)

$$c_s^2 = \frac{c^2}{D}, \quad \nu_p = -\frac{c^2}{2(D+2)}, \quad g(\rho) = \frac{D}{D+2} \frac{b-2\rho}{b-\rho}. \quad (8.11)$$

From eq. (8.9) we can identify the pressure

$$p = c_s^2 \rho \left(1 - g(\rho) \frac{u^2}{c^2} \right). \quad (8.12)$$

The expression for $S_{\alpha\beta}$ in (8.10) is the stress-strain relation for a Newtonian fluid having kinematic viscosity $\nu = \nu_c + \nu_p$ and zero bulk viscosity. The kinematic viscosity has two contributions. The “collision viscosity” ν_c depends on the details of the collision rules and is positive (ref. 42 of FDHLPR). The “propagation viscosity” ν_p is negative; it describes the enhancement of velocity gradients due to propagation on the discrete mesh.

In the hydrodynamic limit ($\epsilon \rightarrow 0$), the resulting equations (FDHLPR eq. 7.13) differ from the Navier-Stokes equations only by the presence of a constant and uniform factor $g(\rho_0)$ in the advection term. This reflects the lack of Galilean invariance at the lattice level. The vanishing of the advection term when $\rho_0 = b/2$ reflects a duality invariance that does not appear in the real world. Still, for $\rho_0 < b/2$ the ordinary incompressible Navier-Stokes equations are recovered by a simple rescaling of time and viscosity:

$$t \leftarrow \frac{t}{g(\rho_0)} \quad \nu \leftarrow g(\rho_0) \nu. \quad (8.13)$$

A tricky point, in the real world as well in lattice gases, relates to the incompressible limit. At low Mach numbers M the density differs from a constant and uniform background, equal to ρ_0 , by small fluctuations $O(M^2)$. To leading order these may be consistently ignored everywhere, except in the pressure term.

Two strategies are available for calculating the viscosity. The fluctuation-dissipation, or noisy hydrodynamics, approach is described in FDHLPR section 8.1. In the next lecture we will use the lattice analogue of the Boltzmann approximation to calculate the velocity explicitly (FDHLPR sec. 8.2).

Frisch #9

**LATTICE GAS HYDRODYNAMICS: REYNOLDS NUMBER,
NOISY HYDRODYNAMICS**

Notes by L. Polvani and B. Dannevik

Today, we shall cover three topics:

1. Evaluation of the viscosity for the lattice gas
2. Maximum achievable Reynolds numbers
3. The influence of thermal noise.

With regard to the determination of viscosity of the lattice gas, we will describe it in general terms, and supply some detail only on the nontrivial parts of the calculation. Viscosity can be estimated by means of various approximations; in most instances, it has been found that the Boltzmann approximation is both appropriate and accurate. The resulting predictions are in very good accord with simulation measurements. The potency of this approach may be related to the possibility that the Boltzmann approximation is not only a low density approximation, but may represent the leading order form of a $1/N$ type expansion. For the lattice gas, the number N would be to the number of cells per node, b .

The Boltzmann approximation reads as follows in terms of the mean populations:

$$\begin{aligned} N_i(t_* + 1, \mathbf{r}_* + \mathbf{c}_i) &= \sum_{ss'} s'_i A(s \rightarrow s') \prod_j N_j^{s_j} (1 - N_j)^{1-s_j} \\ &\equiv N_i^{eq} + \Delta_i, \end{aligned} \quad (9.1)$$

where

$$\Delta_i = \sum_{ss'} (s'_i - s_i) A(s \rightarrow s') \prod_j N_j^{s_j} (1 - N_j)^{1-s_j}. \quad (9.2)$$

When the equilibrium values $N_i = N_i^{eq}$ are substituted into this expression, it is easy to check that the collision terms vanish, as we must expect. To evaluate the viscosity, we use as before multiscale expansion in space and time (to calculate $N_i^{(1)}$, we need only Taylor-expand to linear order). A trick used in Chapman-Enskog procedures is useful here, whereby the lowest-order equation is used to re-express the time derivatives in terms of space derivatives. One of the resulting equations takes the form:

$$\frac{D}{bc^2} Q_{i\alpha\beta} \partial_{i\alpha} (\rho u_\beta) = \sum_j \mathcal{A}_{ij} N_j^{(1)}, \quad (9.3)$$

where

$$\mathcal{A}_{ij} \equiv \left[\frac{\partial \Delta_i}{\partial N_j} \right]_{N_i = \rho/b}. \quad (9.4)$$

This looks like 24 equations in as many unknowns. However, symmetries allow a vast simplification. We may write following Hénon (ref. 42 or FDHLPR, sec. 5):

$$N_i^{(1)} = \psi Q_{i\alpha\beta} \partial_{i\alpha} (\rho u_\beta). \quad (9.5)$$

The system then reduces to a single equation for the scalar function ψ . This permits a closed-form expression for the viscosity (sum of propagation and collision viscosities):

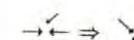
$$\nu = \frac{c^2}{2(D+2)} \frac{\mu}{1-\mu}, \quad \mu = \frac{D}{4(D-1)} \frac{1}{bc^4} \sum_{ss'} A(s \rightarrow s') d^{p-1} (1-d)^{b-p-1} \sum_{\alpha\beta} (Y_{\alpha\beta} + Y'_{\alpha\beta})^2, \quad (9.6)$$

where

$$\begin{aligned} d &= \rho_0/b = \text{reduced density}, \\ p &= \sum_i s_i \\ Y_{\alpha\beta} &= \sum_i \left(s_i c_{i\alpha} c_{i\beta} - \frac{pc^2}{D} \delta_{\alpha\beta} \right). \end{aligned} \quad (9.7)$$

The last quantity has the form of the deviator of a kind of tensor of inertia.

The most interesting part of the present expression for the viscosity relates to the dependence on $Y_{\alpha\beta}$. Note that if the tensor of $Y_{\alpha\beta} + Y'_{\alpha\beta}$ is isotropic for a given collision rule, there is zero contribution to the viscosity. An example is the “head-on collision with spectator”, introduced by D. Levermore:



To get small viscosities, we wish to match in- and out-states to minimize the deviators, subject to the necessary conservation properties. This can be accomplished with optimization algorithms for the “perfect matching” problem. (Actually, we are considering a variant, the “perfect mismatch”, since we wish to minimize the sum $Y_{\alpha\beta} + Y'_{\alpha\beta}$ and not the difference.)

In this manner, a collision table can be worked out which best minimizes the viscosity (Rivet, Hénon, Frisch, and d’Humières, submitted to Europhys. Lett., 1988) In 2-D the best known model is FHP-III (see FDHLPR, sec. 2.2), which includes all possible collisions in a seven-bit model (six with speed-one and one particle at rest).

What are the implications for the resulting Reynolds numbers? The natural unit of length is the lattice constant, and the time unit is the update interval. Recall from the last lecture that the variables which produce the Navier-Stokes equations are scaled as follows:

$$\mathbf{r} = \epsilon^{-1} \mathbf{r}_1, \quad \mathbf{u} = \epsilon \mathbf{U}, \quad \nu = g(\rho_0) \nu'. \quad (9.8)$$

These are the variables in which the Reynolds number R must be formed. Hence,

$$R = \ell_0 u_0 \frac{g(\rho_0)}{\nu(\rho_0)}. \quad (9.9)$$

u_0 is characteristic velocity in natural units of the lattice. It is useful to bring out the Mach number. Thus we write $u_0 = c_s M$ and obtain:

$$R = M \ell_0 R_* (\rho_0), \quad R_* \equiv \frac{c_s g(\rho_0)}{\nu(\rho_0)}. \quad (9.10)$$

For a real fluid, there is evidence from several sources which indicates that compressibility corrections to incompressible dynamics, which scale like $O(M^2)$, are not prominent for $M \lesssim 0.3$. In lattice gases, the scaling is the same, but the constants seem to be more favourable, probably because of the presence of the $g(\rho)$ factor. Typical values chosen for the Mach number M , in lattice gas simulations are thus in the range 0.3 to 0.5.

Note that the function $g(\rho_0)$ is universal for a given lattice, provided that semi-detailed balance is retained. Increasing ℓ_0 is expensive computationally. So, it is worthwhile to expend effort to minimize the viscosity by the strategy outlined previously.

The "Reynolds coefficient" R_*^{max} , the maximum of R_* over the density, is shown hereafter for various models:

	FHP-I	optimal FCHC (pseudo-4-D)
R_*^{max}	0.387	7.57
d_{max}	0.187	0.33

It is necessary to check consistency conditions for our formulation, in terms of the required scale separation (i.e., we must check that our ϵ is acceptable). A necessary condition is that the dissipation scale be large compared with the lattice constant. We can check this in the following way. In a turbulent flow, the ratio of dissipation scale η and integral scale ℓ_0 is:

$$\frac{\eta}{\ell_0} \sim CR^{-m} \left\{ \begin{array}{l} m = 3/4 \quad (3\text{-D}), \text{ according to Kolmogorov 1941} \\ m = 1/2 \quad (2\text{-D}), \text{ according to Batchelor-Kraichnan.} \end{array} \right. \quad (9.11)$$

So, we find for the dissipation scale the following estimates:

$$\eta = \begin{cases} C(MR_*^{max})^{-1/2} \ell_0^{1/2} & (2\text{-D}) \\ C(MR_*^{max})^{-1/4} \ell_0^{1/4} & (3\text{-D}). \end{cases} \quad (9.12)$$

We stress again that the dissipation scale η is here measured in lattice constants (=meshes). As we aim for high Reynolds numbers, η will quite large, thereby ensuring the separation of scale required for the validity of the hydrodynamic approximation. Actually, for computational efficacy, it is of interest to reduce η by increasing R_*^{max} : a gain of a factor 2 on R_*^{max} amounts to a computational gain of a factor 8 in two dimensions and of a factor 16 in three dimensions.

We have stated that a separation of scale between micro- and macro-worlds is necessary for hydrodynamics, but it may not be sufficient. The following analysis has been worked out in collaboration with V. Yakhot and S. Orszag. We shall show that, at high Reynolds numbers, there is actually a kind of breakdown of the hydrodynamics in the dissipation range: microscopic noise terms must be added to the incompressible Navier-Stokes equations. The subsequent analysis applies equally well in lattice gases and in the real world, provided the density is $O(1)$ (with the mean free path as unit length).

We already know from the Kolmogorov 1941 theory in 3-D and the Batchelor-Kraichnan theory in 2-D that incompressible fluid velocity fluctuations are very small at small scales. Hydrodynamic pressure fluctuations are even smaller since they scale like the square of the former. Maybe they become so small that microscopic fluctuations dominate. Using the mean free path as unit length and the thermal velocity as unit speed we obtain kinematic viscosities ν which are $O(1)$ (we here ignore subtle divergence effects which could be present in 2-D). The dissipation scale η , in any dimension is characterized by its turnover time $t_\eta \sim \eta/v_\eta$ equal to the viscous diffusive time $t_\eta^{diff} \sim \eta^2/\nu \sim \eta^2$. Thus $v_\eta \sim 1/\eta$ and $t_\eta \sim 1/\eta^2$. Typical hydrodynamic (macroscopic) turbulent fluctuation of the pressure (actually of pressure/density) are

$$P_\eta^{macro} \sim v_\eta^2 \sim 1/\eta^2. \quad (9.13)$$

Microscopic fluctuations must be evaluated averaged over a space-time domain of spatial extent η and temporal extent t_η . Spatially there is essentially no microscopic coherence so that relative fluctuations can be estimated by the usual $1/\sqrt{N}$ argument ($N = \eta^D$ being the number of particles in a box of size η). The temporal coherence of pressure fluctuations is the time necessary for a sound wave to propagate over a distance

η , that is $t_\eta^{\text{sound}} \sim \eta$. Thus there are $O(\eta)$ such coherence times in t_η . This results in an additional lowering factor of $1/\sqrt{\eta}$ in the relative spatio-temporal fluctuations. Hence the expected relative density (or pressure) fluctuations of microscopic origin should be

$$P_\eta^{\text{micro}} \sim \frac{1}{\eta^{D/2}} \cdot \frac{1}{\eta^{1/2}} \sim \eta^{-\frac{1+D}{2}}. \quad (9.14)$$

Comparisons of eqs. (9.13) and (9.14) shows that in two dimensions the microscopic noise in the pressure swamps the hydrodynamic signal (recall that η measured in units of mean free path is large!). This argument of course applies only in "Flatland", a country which is 2-D, even microscopically. In three dimensions, we find that microscopic fluctuations of the pressure are just about equal to the hydrodynamic signal at the dissipation scale.

A random noise term of microscopic origin should therefore be added to the Navier-Stokes equations to accomodate the microscopic fluctuations, as discussed in sec. 8.1 of FDHLPR. This additional noise term has the form of an inhomogeneous forcing term which is a gradient. Therefore, it does not directly affect the dynamics of the velocity field in the incompressible limit. The above analysis can be modified to estimate fluctuations of the incompressible (solenoidal) velocity which are of microscopic origin (Ruelle, Phys. Lett., **72A**, 81, 1979). Such fluctuations are very small and become relevant only in the far dissipation range. Still, at moderately small Mach numbers M , pressure fluctuations of microscopic origin will contaminate solenoidal velocity fluctuations (by $O(M^2)$ terms). We can therefore expect a breakdown of the usual noiseless hydrodynamics not very far out in the dissipation range. Such questions require further study. Here, we just mention that noise-contamination should have implications for the predictability issue in strongly-turbulent flows.

LATTICE GAS HYDRODYNAMICS: SOFTWARE AND HARDWARE IMPLEMENTATIONS. CONCLUDING REMARKS

U. Frisch

We here give just an outline of implementation questions; for details, see Refs. 31 and 34 of FDHLPR. Boundary conditions are easy to implement at the microscopic level. As already stressed by Maxwell, walls are not microscopically "flat": molecules are diffusely reflected in such a way that the average velocity vector is (usually) zero at the wall. In practice, in lattice gas calculations, one implements the no-slip condition by bouncing back the particles from the boundary nodes. The free-slip boundary condition is obtained by a specular reflection. In- and out-flow conditions, which can be quite tricky to implement in traditional methods, are easily handled in lattice gas calculations through particle injection and removal; in this way one can design a lattice gas wind-tunnel. Since boundary nodes represent usually a very small fraction of all the nodes, the computational overhead from incorporating boundaries is typically only a few percent.

The density (i.e. mean number of particles per node) is an important parameter that affects the viscosity (and hence the maximum achievable Reynolds number) of a lattice gas CA. The maximum hydrodynamic velocity must be adjusted with care. If it chosen to be too small, the Monte-Carlo noise will swamp the macroscopic signal and the Reynolds number will be comparatively small. If the velocity is too large (i.e. the Mach number is too high) compressibility effects and spurious higher-than-quadratic nonlinearities cannot be neglected. Adjusting the hydro-velocity is an art (that is, not easily codified by rigid rules). In traditional floating point calculation, using for example spectral methods, comparable craftsmanship is required in adjusting the viscosity: too large, resolution is wasted, and too small, truncation errors become severe.

In order to be confident of the Reynolds number at which one is operating the CA, it is desirable to know the value of the viscosity. It can be calculated using the Boltzmann approximation, or measured by simulating the decay of a single Fourier-mode, either a compressible mode (sound-wave) or a shearing mode. Comparison with the expected exponential damping (time-variation like $\exp(-\nu k^2 t)$) gives an estimate for the viscosity ν .

To extract the hydro-velocity, space-time averaging over "mesoscopic" domains is required. By "mesoscopic" we understand large compared to microscopic distances (the lattice constant) and small compared to macroscopic distances (the integral scale for the velocity and the dissipation scale for the vorticity and other space-derivatives). Time

averaging is often found to be unnecessary for the velocity. Space averaging can be done by just adding the microscopic velocities of all the nodes within mesoscopic cells, or by more fancy filtering techniques, e.g. Fourier-space filtering which is particularly useful for getting derivatives.

In software simulations of lattice gases, the updating is done in two steps: collision (including boundary-node update) and propagation. There are two basic strategies for software implementation of a lattice-gas CA. The first (storage by node) consists in storing the nb bits corresponding to the b different permitted microscopic velocities of n nodes into a same memory word. The second strategy (storage by velocity) consists in storing in one memory word bits pertaining to identical microscopic velocities of different nodes, usually consecutively located on the lattice. Storage by node allows an easy solution for the collision phase: the b -bit out-state (after collision) of a given node is fetched from a look-up table of $b \times 2^b$ bits with the in-state as address; several tables are used if the collision rules involve a random element. With storage by node, propagation requires the moving of the various bits of a word into different directions; this may be operation-intensive. Storage by velocity renders propagation very easy: it just amounts to a shift; however, collisions become more difficult to implement by look-up table, since the b bits of a given node must first be assembled from different memory words. General purpose computers may not have the hardware to do this in a small number of clocks. An alternative to look-up tables is "collision by Boolean logic". This is best illustrated by considering the HPP lattice. The collision rule is then that the states $(1, 0, 1, 0)$ and $(0, 1, 0, 1)$ are to be interchanged and that all other states are unaffected. A brute force Boolean logic implementation is provided by the r.h.s. of eq. (6.5). This requires $4 \times 13 = 52$ operations. However, an equivalent formulation of the HPP collision rule is "if the first bit is different from the second bit and the second bit is different from the third bit and the third bit is different from the fourth bit, then negate all the bits, otherwise leave them as they stand". Using the **XOR** and the **AND** logical operations, this can be implemented in only 9 operations. In general, one can start from a brute force logical expression of the collision operator and apply "Boolean reduction", that is find an equivalent Boolean expression involving a minimum number of operations. Unfortunately, Boolean reduction is a very complex problem (somewhat like the travelling salesman problem) and no efficient systematic Boolean reduction schemes are known. Choosing among the various above strategies depends very much on specific architecture details of the machine on which the software implementation is done. For

example, if the machine has a very large common memory, as on CRAY-2's and some CRAY-XMP's, very efficient implementations of the pseudo-4-D model can be made, using an optimized collision look-up table with 2^{24} entries (Rivet, Hénon, Frisch, and d'Humières, submitted to Europhys. Lett., 1988).

Existing computers (particularly the so-called supercomputers) are usually optimized for floating point calculations. For CA calculations it may be better and/or cheaper to use specially designed hardware. This is the case of the MIT Cellular Automaton Machine (CAM, see ref. 8 of FDHLPR) and of Ecole Normale Supérieure's Réseau d'Automates Programmable (RAP, see ref. 34). RAP-1, which has been optimized for 2-D lattice gas calculations on 256×512 nodes with up to 16 bits per node, runs at a speed which is a sizeable fraction of the best known CRAY-1 software implementation (depending on the specific model). It displays hydrodynamic phenomena in real time (50 complete lattice updates per second). The cost of its off-the-shelf hardware components is about one thousand dollars. Larger 2-D machines, also operating in real time, but able to handle lattices several thousands by several thousands are now being built. Their cost may be compared to that of a mini-computer. Based on the acquired experience with 3-D simulations, designs for 3-D hardware are now being considered.

We mention that lattice gas models can be constructed to handle free-boundary flows, multi-phase flows and combustion (see refs. 56 and 57). Keeping a sharp interface between two non-mixing species can be tricky in traditional methods. Introducing a microscopic level, allows easy solutions. One way to keep molecules *A* and *B* segregated is to have a majority rule, such as $2A + B \rightarrow 3A$ and $2B + A \rightarrow 3B$. Segregation with interfacial tension has recently been achieved by Rothman and Keller (preprint, Dep. Earth Sci., MIT, 1987). Combustion phenomena can be simulated by having chemical reactions between species releasing heat (this requires a multi-speed model). Another potentially interesting domain of application of lattice gas methods is cavitation, because of its two-phase flow aspects and also because there are connected problems of sound generation.

Lattice gas methods are now becoming competitive with floating point methods for certain applications. For example, the simulation of transition to full three-dimensionality in flows past obstacles with symmetries (Rivet et al., 1988). Still, unrestrained enthusiasm would be inappropriate. Floating point methods are usually a lot more flexible than lattice gas methods; considerable inventiveness being required for the latter, whenever new phenomena are to be introduced (e.g. surface tension). Furthermore, floating point

methods have benefitted from about half a century of development. It is thus desirable to develop mixed approaches combining the advantages of both methods.

What can we hope to learn about turbulence from lattice gas simulations? This may depend on how crucial it is to have realistic boundaries. Complex boundaries are easy to implement in lattice gas calculations. High Reynolds numbers simulations with simple or trivial (periodic) boundary conditions are presently most efficiently achieved by *spectral methods*. One view common among statistical turbulence theorists, is that turbulence at very high Reynolds number is sufficiently universal that it forgets about the details of the boundaries. According to this view, we may simulate the essential features of very high Reynolds number turbulence by running on a supercomputer a spectral code with periodic boundary conditions at the highest possible Reynolds numbers.

Another view is that without boundaries we may not even be capturing the fine-scale structure correctly, i.e. we are throwing out the baby. At transitional and moderately high Reynolds numbers, boundaries are clearly essential. We cannot rule out that this remains true at very high Reynolds numbers. The traditional picture of fully developed turbulence has the fine-scale structure generated by a cascade process, starting at the most energetic scales. We know, however, that vorticity, a key to understanding the fine-scale structure, usually originates from detached boundary layers generated at the walls. Putting vorticity "by hand" at large scales, as in Taylor-Green simulations, may or may not make a difference. Experimental results obtained in Chicago on turbulent convection at Rayleigh numbers up to 6×10^{12} tend to support the view that keeping realistic boundaries is essential (Castaing, Gunaratne, Heslot, Kadanoff, Libchaber, Thomae, Wu, Zalesky, and Zanetti, "Scaling of hard thermal turbulence in Rayleigh-Bénard convection", preprint Res. Institutes, Univ. Chicago, 1988). This may however be so because the Chicago experiment has not yet attained a fully developed turbulence regime.

Turbulence is at this moment an undefinable concept and is likely to remain so as long as it is considered interesting. We must be prepared to accept that turbulence presents a mixture of universal and non-universal features. It may even have a complexity comparable to that of biological structures. We do not know what will provide the "crucial" data needed for the theory. Simulations (floating point and lattice gas) allow a very detailed analysis of moderately turbulent flows. Experiments have no difficulty achieving very high Reynolds number, but flow control and visualization can become major challenges. All avenues should be tried.